

Aim and Scope

The objective of the *Journal of Residuals Science & Technology* (JRS&T) is to provide a forum for technical research on the management and disposal of residuals from pollution control activities. The Journal publishes papers that examine the characteristics, effects, and management principles of various residuals from such sources as wastewater treatment, water treatment, air pollution control, hazardous waste treatment, solid waste, industrial waste treatment, and other pollution control activities. Papers on health and the environmental effects of residuals production, management, and disposal are also welcome.

Editor-in-Chief

P. Brent Duncan
Department of Biology
University of North Texas
Denton, TX, USA
pduncan@unt.edu

Editorial Advisory Board

Muhammad Abu-Orf
AECOM, USA
mohammad.abu-orf@aecom.com

Steve Dentel
University of Delaware, USA
dentel@udel.edu

Richard Dick
Cornell University, USA
rid1@cornell.edu

Guor-Cheng Fang, Ph.D.
Hungkuang University, Taiwan
gcfang@sunrise.hk.edu.tw

Robert Hale
Virginia Institute of Marine Science, USA
hale@vims.edu

Paul F. Hudak
University of North Texas, USA
hudak@unt.edu

Blanca Jimenez Cisneros
Inst. de Ingenieria, UNAM, Mexico
bjc@mumas.iingen.unam.mx

Julia Kopp
Technische Universitat
Braunschweig, Germany
j.kopp@tu-bs.de

Uta Krogmann
Rutgers University, USA
krogmann@aesop.rutgers.edu

D. J. Lee
National Taiwan University, Taiwan
djlee@ntu.edu.tw

Giuseppe Mininni
Via Reno 1, Italy
mininni@irsa.rm.cnr.it

John Novak
Virginia Tech, USA
jtnov@vt.edu

Rod O'Connor
Chemical Consulting Services, USA
docroc34@hotmail.com

Nagaharu Okuno
The University of Shiga Prefecture,
Japan
okuno@ses.usp.ac.jp

Jan Oleszkiewicz
University of Manitoba, Canada
oleszkie@ms.umanitoba.ca

Banu Örmeci
Carleton University, Canada
banu_ormeci@carleton.ca

Ian L. Pepper
University of Arizona, USA
ipepper@ag.arizona.edu

Ioana G. Petrisor
Co-Editor-in-Chief
Environmental Forensics Journal, USA
Environmental.Forensics@gmail.com

Bob Reimers
Tulane University, USA
rreimers@tulane.edu

Dilek Sanin
Middle East Technical University,
Turkey
dsanin@metu.edu.tr

Mike Switzenbaum
Professor Emeritus
Marquette University, USA
michael.switzenbaum@marquette.edu

Heidi Snyman
Golder Associates Africa (Pty) Ltd.,
South Africa
hsnyman@golder.co.za

Ludovico Spinosa
Consultant at Commissariat
for Env. Energ. in Region,
Puglia, Italy
ludovico.spinosa@fastwebnet.it

P. Aarne Vesilind
Bucknell University, USA
aarne.vesilind@gmail.com


Doug Williams
California Polytechnic State
University, USA
wmsengr@thegrid.net

JOURNAL OF RESIDUALS SCIENCE & TECHNOLOGY—Published quarterly—January, April, July and October by DEStech Publications, Inc., 439 North Duke Street, Lancaster, PA 17602.

Indexed by Chemical Abstracts Service. Indexed/abstracted in Science Citation Index Expanded. Abstracted in Current Contents/Engineering, Computing & Technology. Listed in ISI Master Journal.

Subscriptions: Annual \$219 per year. Single copy price \$60. Foreign subscriptions add \$45 per year for postage.

(ISSN 1544-8053)

 DEStech Publications, Inc.

439 North Duke Street, Lancaster, PA 17602-4967, U.S.A.

©Copyright by DEStech Publications, Inc. 2013—All Rights Reserved

C O N T E N T S

Research

- Municipal Sewage Sludge Management in the Slovak Republic—Actual Status and Perspectives**153
IGOR BODÍK and MIROSLAVA KUBASKÁ
- Present and Future Sewage Sludge Treatment in Hungary and its Energetic Utilisation**161
FERENC ZSABOKORSZKY
- Modeling of Wastewater Sludge Drying with Determination of Diffusivity Moisture**165
L. BENNAMOUN, L. FRAIKIN, T. SALMON, M. CRINE and A. LÉONARD
- Penetrant Liquid Waste Degradation by Radiocatalysis**171
JAIME JIMÉNEZ-BECERRIL, JULIO CÉSAR GONZÁLEZ-JUÁREZ and
ROBERTO CONTRERAS-BUSTOS
- Hydrothermal Carbonization of Organic Material with Low Dry Matter Content:
The Example of Waste Whey**179
M. ESCALA, A. GRABER, R. JUNGE, CH. KOLLER, V. GUINÉ and R. KREBS
- Preparation of High-Specific Surface Area-Activated Carbon with Oil-Bearing Mud Residue**187
YUE MA, MIAN CHEN and YAN JIN

Municipal Sewage Sludge Management in the Slovak Republic— Actual Status and Perspectives

IGOR BODÍK* and MIROSLAVA KUBASKÁ

*Department of Environmental Engineering, Faculty of Chemical and Food Technology, Slovak University of Technology,
Radlinského 9, 812 37 Bratislava, Slovakia*

ABSTRACT: Status of municipal sewage sludge management in the Slovak Republic is reviewed herein. Eighty-six point nine percent of the Slovak population is connected to water supply and sixty-one point six of the Slovak population connected to wastewater collection systems. During 2010 total sludge production in Slovakia was 58,718 ton (TS). More than 75% of sludge produced was anaerobically digested and about 85% was applied to agricultural soils. Total volume capacity of anaerobic digestion tanks in WWTPs is 195,000 m³ with daily biogas production more than 60,000 m³. CHP units were installed in 21 plants with total electric output at 5.4 MW_e and total electric production at more than 67,000 kWh_e/day.

INTRODUCTION

WASTEWATER TREATMENT PLANTS (WWTP) are important components of environmental protection all over the world. Increasing waste and wastewater production creates pollutant by-products that may contaminate surface, as well as subsurface water. Organic pollution in wastewater is partly separated as primary sludge during the mechanical stage of the plant and also partially transformed into activated sludge during the biological part of the WWTP process. All types of wastewater treatment technologies inevitably generate sludge. Production of sludge from wastewater, and the need for treatment of sludge, and subsequent need to dispose the sludge has been viewed as a serious solid waste management problem incurring financial costs [1,2].

There are many possibilities on how to treat sludge: aerobic sludge stabilisation, chemical sludge stabilisation (mainly for small WWTPs), sludge incineration (used if an available incineration plant is within an appropriate distance), and anaerobic digestion. Anaerobic digestion of treatment sludge has received much attention in recent years as a means of generating biogas that in turn may be used to generate energy with combined head and power (CHP) units. Operators of WWTPs are finding adoption of sludge treatment technology is economically feasible. Many large WWTPs

around the world are shifting operation modus of sludge management into anaerobic sludge digestion with biogas and consequently electric energy production (e.g., Vienna). Advantage of CHP implementation is generated electricity that is both directly usable on-site for energy demands for equipment (e.g., aeration, pump, mixing) and/or that may be re-sold to the public economically speaking [3].

Biogas is generally produced in landfills, biogas plants, and WWTPs by anaerobic microorganisms during anaerobic fermentation of organic material. Biogas produced in WWTPs and in biogas plants for agricultural and municipal purposes is generally used for energy production both thermal and electric. Thus, due to increasing interest in renewable energy sources biogas has become a notable alternative to conventional fuels used for production of electricity and heat.

Water Management System in the Slovak Republic

Slovak Republic is located in the middle of Central Europe. The actual number of inhabitants in the Slovak Republic is about 5.44 million (2011). Total number of settlements in the country is 2,891. Only 400 settlements have more than 2,000 inhabitants. Total number of inhabitants living in towns with more than 2,000 inhabitants is 3.78 million. This represents about 70% of the population. The rest of the population is spread into small settlements over the remaining Slovakian territory. Above all the aforementioned geographical facts, the high proportions of rural populations create com-

*Author to whom correspondence should be addressed.
E-mail: igor.bodik@stuba.sk

plicated conditions related to connecting populations to central water supply systems and for wastewater treatment systems and also in accordance with documents of the Slovak Republic into EU from 2004 [4]. Broadly disperse populations is a primary reason for a centralized water distribution system and wastewater treatment system review by the EU with Slovak Republic member requirements [4].

The number of inhabitants supplied with drinking water from the public water supply in 2010 reached 4.72 million and represents 86.9% of total inhabitants. Total length of drinking water pipelines was 28,777 km and represents a specific length of pipeline on connected inhabitant 6.09 m. There are 2,353 Slovak Republic individual municipalities supplying drinking water. Ground water resources produced 270 million m³ of drinking water representing 84.2% of water derived from surface water resources. Water losses in pipeline systems represented very high figures (e.g., 28.5% from total water produced in the Slovak Republic). Specific water consumption for households dramatically decreased from 195 L/cap.d in 1990 to 79.8 L/cap.day in 2011 [4].

Development of public sewage systems lags behind that of public water supply systems. Connection percentage in the Slovak Republic is relatively low in comparison to developed countries in Western Europe. This dates back to long-term neglected development of infrastructure construction projects during the communist era for all CEE countries. Number of inhabitants living in households connected to public sewage systems reached 3.35 million inhabitants and is 61.6% of the Slovak population. Total length of sewage system pipelines was 11,211 km. It represents a specific length of pipeline on connected inhabitant 3.35 m. Average water price in Slovakia was 2.31 €/m³ for both water supply and treatment [4].

Wastewater Treatment Plants

During 2011, 616 municipal WWTPs with a total capacity of 2.1 Mil.m³/day treated 1.32 Mil.m³/day or 62.9% of capacity. The main portion of technological structures represents mechanical-biological plants with 93.5% of all operated plants. According to requirements from EU Directive 91/271/EHS and also according to statistical related evidence from Slovak WWTPs the geographical system of 356 agglomerations with more than 2,000 p.e. was created from which 284 WWTPs are today still operated. Regarding this number of WWTPs only 269 plants fulfilled EU Directive

Table 1. Distribution of Capacity Groups of WWTPs in the Slovak Republic [4].

WWTP Capacity Groups	Operated WWTPs	% Population Served
< 2000 p.e.	332	15.0
2001–10 000 p.e.	203	41.8
10 001–15 000 p.e.	18	68.5
15 001–150 000 p.e.	58	82.3
>150 000 p.e.	5	92.4
Total	616	61.6

effluent requirements for organic pollution and only 46 plants (more than 10,000 p.e) fulfilled nutrient requirements.

The fifty largest Slovak WWTPs have a design capacity for more than 6.9 million p.e. However, the true load is greater than 2.8 million p.e. The purpose for unused high design capacity is a sharp decrease in the industrial pollution portion of municipal wastewater load in the past ten-twenty years. Total flow for the fifty largest WWTPs is more than 800,000 m³/day which represents 60% of all Slovak WWTPs flow. The largest Slovak WWTP is Central WWTP in Bratislava with a treatment capacity of 1.06 million p.e. and with an actual load of 360,000 p.e. representing about 15% of total Slovak wastewater load and flow, respectively.

Sludge Management System in the Slovak Republic

Sewage sludge is waste, and sludge management in the Slovak Republic is generally regulated by legislation valid for waste management respecting requirements for *acquis communautaire* for this area [5]. There are two basic policy documents used for control of sludge application onto soils as follows:

- Direct application of sludge into soil according to Act no.188/2003 Coll. on application of waste water sludge into soil, and
- Application as of Act no. 136/2000 Coll. in wording of Act no.555/2004 Coll. on fertilizers (e.g., as compost or soil-growing medium). In this case the product is subject to certification.

Amount of sludge produced in municipal WWTPs is permanently monitored and recorded. Yearly municipal sludge production in the last few years is about 54,000–58,000 t (TS) which represents average specific sludge production at approximately 16.7 kg/p.e.year. In

Table 2. Sludge Production in the Slovak Republic and the Ways of Its Utilisation [4].

Year	Total	Sludge Production (in tons of dry solids)				
		Direct Soil Application	Composted	Landfilled	Incinerated	Others
2002	52,149	42,836	0	4,443	0	4,870
2004	53,085	12,067	30,437	4,723	0	5,858
2006	54,780	0	39,405	9,245	0	9,400
2008	57,810	0	38,368	8,676	0	10,766
2009	58,582	0	47,056	2,696	0	8,830
2010	54,760	923	47,140	16	0	6,681
2011	58,718	358	50,111	2,306	0	5,943

Table 2 there are data about sludge production and ways of sludge utilisation. Approximately, 90% of sludge is stabilised by anaerobic digestion in 52 WWTPs. The rest uses aerobic sludge stabilisation technology (low loaded activated sludge systems). Chemical (lime) stabilisation is rarely used.

According to data in the literature it is evident that indirect soil application of sludge as compost is the most frequent way (i.e., about 85%) of sludge disposal. Formerly, the often used method of direct sludge application in soil was extremely reduced according to strict requirements for sludge quality. Decrease of landfilled sludge is also evident during the last few years. This tendency probably will continue.

There are two techniques for regulated application of sewage sludge applied to agricultural lands:

- Direct application of sludge onto agricultural land according to Act No.188/2003 on Sewage Sludge Application onto Agricultural Land, determining conditions for sewage sludge application onto agricultural and forest land without affecting soil properties, plants, water, human health, and animals [6]. Sludge application must be approved by the authority of agricultural land resources protection or by authority of a forest management state administration. The act with certain hygienic and time limitations enables agriculture related application on permanent grass stands. It does not deal with application onto non-agricultural related lands or sludge use in land reclamation.
- Application in line with Act No.136/2000 on Fertilizers (e.g., compost) regarding soil supporting substance or growing medium. In this case, the product made on the basis of sludge is subject to certification and assessment whether properties of such fertilizer and its technical documentation are in line with related technical standards and generally binding legal regulations.

Incineration of municipal treatment sludge is not used in Slovakia (on-site incineration of sludge occurs at two industrial WWTP's, DUSLO Šaľa and Slovnaft Bratislava. There are no suitable incineration capacities for sludge incineration. There are some newer ideas about incineration of sludge but only in project preparation studies. Generally, the attitude (public and "green NGO's") towards waste incineration is very negative in the Slovak Republic.

Technologies of Sludge Treatment Used in the Slovak Republic

Aerobic sludge stabilisation technology is operated predominantly on small WWTP's with a load capacity below 10–15,000 p.e. There are about 550 small facilities and only two large WWTPs (Ružomberok at 325,000 p.e. and Rimavská Sobota at 32,000 p.e., respectively) with this type of system for sludge stabilisation. Yearly production of aerobically stabilised

Table 3. Limits for Application of WWTP Sludges onto Agricultural Land [4].

Parameter	Concentration Limit mg/kg TS	Load Limit g/ha.year
As	20	60
Cd	10	30
Cr	1000	3000
Cu	1000	3000
Hg	10	30
Ni	300	900
Pb	750	2250
Zn	2500	7500
PAH	6.0	–
PCB	0.8	–
AOX	500	–
	CFU/g TS	
Thermotolerant coliforms	2.10 ⁶	–
Faecal streptococci	2.10 ⁶	–

sludge is approximately 20–25% from total sludge production using Slovak municipal sludge. According to relatively good sludge quality for WWTPs for small villages and towns without industrial pollution, this sludge may be applied to agricultural soil directly or indirectly as compost.

Anaerobic sludge digestion with biogas production and utilisation is realised on 51 municipal WWTPs with about 2.6 million connected p.e. About 75–80% of Slovak treatment sludge is produced from these plants. The smallest WWTPs with anaerobic sludge digestion are operated in a load range below 10,000 p.e. (Veľký Krtíš at 6,000 p.e., Bytča at 7,500 p.e., Handlová at 9,000 p.e., and Myjava at 9,000 p.e.). Of course, all these small WWTPs have a design capacity much higher at 15–25,000 p.e.

All large Slovak WWTPs except the two previously mentioned are operated with anaerobic sludge digestion under mesophilic conditions. Most monitored plants are operated under a temperature range between 37–39°C, but there are also some digesters using 35°C and 42°C. There is no WWTP with thermophilic anaerobic sludge stabilisation. However, there are some ideas for applying this technology on some plants in the near future.

From a technological point of view Slovak digesters are two-staged reactors with mesophilic digestion occurring during the first stage. The second stage is operated as an open sludge storage reactor without a temperature controlled regime and also without biogas ex-

hausting. Most digesters were constructed in 70–80's and have a "classic" cylindrical shape (see Figures 2 and 3).

Total volume capacity for digestion tanks in these WWTPs is about 195,000 m³. The smallest is 600 m³ and the largest is 30,000 m³. It appears specific volumes (SV) for digestion tanks (Litre/p.e.) are relatively high and this appeared obvious after study of volume of digestion tanks responding to one connected p.e. Average value is 74 L/p.e., the smallest value of SV was measured in the WWTP Bánovce n/Bebravou (22 L/p.e.) and the highest value of SV was achieved in the WWTP Veľký Krtíš (185 L/p.e.). See Figure 4. There are 12 plants with specific volumes of digestion higher than 100 L/p.e. that in most cases assign non-effective operation of sludge management. Regarding comparison to Slovak specific digester volumes, large digesters in European municipal WWTPs are significantly smaller (e.g., Hague at 30 L/p.e., Berlin Schöner. at 38 L/p.e., Madrid at 33 L/p.e., and others). On the other hand, the European WWTPs with thermophilic digesters (e.g., Prague, Budapest, Pilsen, and Braunschweig) have specific digester volumes much smaller at 18–25 L/p.e. [7].

A very important technological parameter concerning economic and energy operation effectiveness of digestion tanks is hydraulic retention time (HRT) of sludge in a digestion tank. Average HRT of sludge in digestion tanks with or without storage tank is about 35 days and varies between 15 to 77 days. Also, these



Figure 1. Slovak municipal WWTPs with anaerobic digestion.



Figure 2. WWTP Trnava at 211,000 p.e.



Figure 3. WWTP Lučenec at 20,000 p.e.

technological parameters similar to specific volume of digestion tank indicate that most WWTPs are over-dimensioned or insufficiently charged. Data in the literature and operations experience point out that optimal HRT is approximately 20 days and an increase of this parameter could cause lower efficiency of organic matter decomposition [8].

The high retention time in the Slovak WWTPs is caused by relatively low TS content in the sludge upon input into digesters at 3–3.5%. These values indicate a low efficiency of sludge thickening processes or low interest about energetic/thermal balances of digester reactors. The low TS content in influent sludge has important consequences regarding high heat losses for raw sludge heating. Thermal balances for digestion process could be much more effective with higher raw sludge content (4–7%) upon input into digesters [9]. Two largest Bratislava WWTPs have average TS

content of raw sludge after thickening in the range between 2.5–3.5%. Therefore, the organic load of digesters is also low at 0.7–0.9 kgVSS/m³.day. Twenty large European WWTPs under operation of VEOLIA WATER have raw sludge concentration on average at 4.8% (Hague at 6.0%, Prague at 5.0%, Madrid at 4.9%, Pilsen at 4.7%, and more) [7].

Biogas Production in Slovak WWTPs

In the year 2011 more than 60,000 m³ of biogas were produced from Slovak municipal WWTPs daily. That represents an annual production of almost 22 million m³ of biogas and theoretically more than 131 GWh of energy bounded in biogas. There are some plants with relatively low daily biogas production—below 200 m³/day. However, there are also WWTPs with 3–4,000 m³/day. The highest biogas production for a

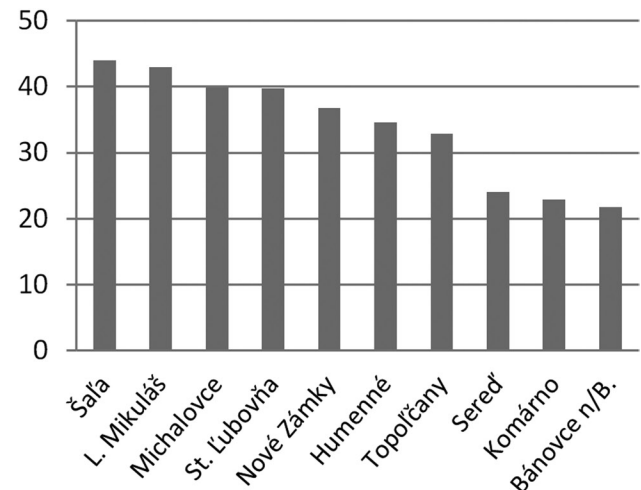
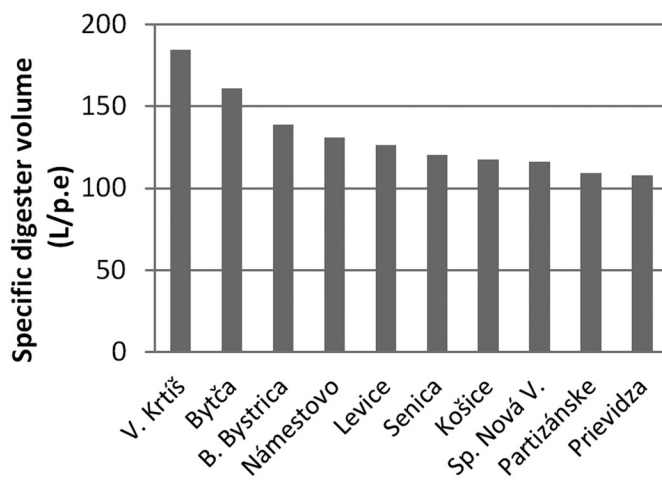


Figure 4. Slovak WWTP with highest and lowest specific digester volume.

WWTP is in Central Bratislava at 13,500 m³/day. The value of specific biogas production (litre of biogas/p.e. connected) is important to compare biogas production efficiency among different plants. These data in Slovak WWTPs varies between 8 L/p.e. (WWTP Topolčany at 30,000 p.e.) and 46 L/p.e. (WWTP Michalovce at 40,000 p.e. without a CHP unit) with average values for all examined Slovak WWTPs at 21 L/p.e. Figure 5 displays specific biogas production for 10 WWTPs with highest biogas production. Values of specific biogas production could be affected by adding external co-substrates for some plants with the aim of biogas production increasing.

Regarding comparison to European large WWTPs, biogas production values are unfavourable for Slovak plants. Twenty EU plants have on average 28 L/p.e. (Seafield at 45 L/p.e., Hague at 27 L/p.e., Madrid at 23 L/p.e., and more) which is about 30% higher specific production than production in Slovak plants. Interesting is that four thermophilic digester operation (Prague, Budapest, Pilsen, and Braunschweig) created slightly lower specific biogas production (26 L/p.e.) in comparison to mesophilic ones. However, specific biogas production for the largest Slovak WWTP Bratislava Central is relatively high at 39 L/p.e. in comparison to other metropolitan WWTPs: Prague at 25.2 L/p.e. (with thermophilic digestion), Berlin at 25 L/p.e., Hague at 27 L/p.e., Madrid at 23 L/p.e., and more. [7].

Only 23 of 51 WWTPs have installed equipment for electrical power production (CHP) with a total installed output of 5.4 MW_{el}. Individual WWTPs have a performance range of 35–1,660 kW_{el}. In 2011 all WWTPs discussed here had daily production of

67,000 kWh of electrical power representing 24.5 GWh annually. Efficiency of biogas utilisation for electric energy production was relatively low at 1.2 kWh_e/m³ of produced biogas in comparison to VEOLIA plants at 2.0 kWh_e/m³. Some Slovak WWTPs have very low profitability regarding electric energy production at 0.2 kWh_e/m³ (Poprad at 115,000 p.e. and Prešov at 85,000 p.e.) because of preferred utilisation of biogas for digester heating in northern/mountain parts of Slovakia.

Energy from self-produced electric sources in Slovak WWTPs was on average approximately 26% with ranges for individual WWTPs from 2–68%. The highest energy autarky was the Central WWTP Bratislava at 66% (co-fermentation of technical fats) and WWTP Trnava at 58% (no co-fermentation). Some European WWTPs with biowastes' co-fermentation achieve energy autarky up to 80–100% (Budapest, Braunschweig, Grevesmühlen) [7].

From a technological point of view, digestion tanks have a sufficient capacity for a considerable increase in biogas production [10]. The increase may be achieved by sufficient choice and dosage of external organic sources that may provide a significant energy—economic contribution to WWTP operations without need for technological process adaptation (e.g., plant oils, fats, and organic materials) or with a small technological process adaptation (food residues, food and agricultural products and wastes). In cooperation with municipalities biogas treatment with bio-fuel production for public transport seems to be very interesting. According to information from water companies many WWTPs have a serious interest regarding installation of or enlargement of electrical power production.

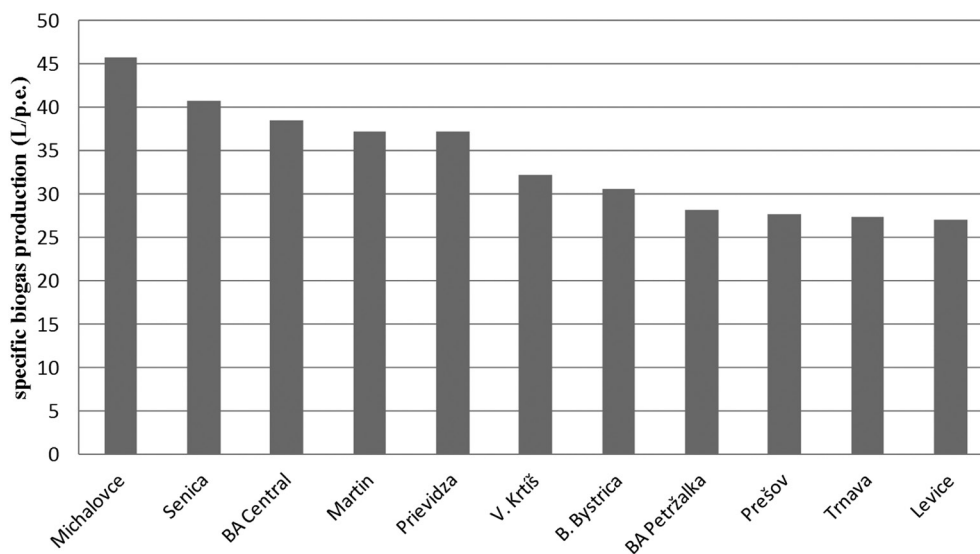


Figure 5. Slovak municipal WWTPs with highest specific biogas production.

CONCLUSION

Development of public sewage systems lags behind public water supply systems. Connection percentage in the Slovak Republic is relatively low in comparison to developed countries of Western Europe. According to requirements of EU Directive 91/271/EHS and also according to statistical evidence from Slovak WWTPs the geographical system of 356 agglomerations with more than 2,000 p.e. was created from which 284 WWTPs are operated today. From this number of WWTPs only 269 plants fulfilled EU Directive effluent requirements for organic pollution and only 46 plants with more than 10,000 p.e fulfilled nutrient requirements. Status of sludge management in the Slovak Republic is comparable to other EU countries and in compliance with EU Directives.

Anaerobic sludge digestion with biogas production and utilisation is realised for 51 municipal WWTPs with daily biogas production more than 60,000 m³ and with specific biogas production 21 L/p.e. Increasing utilisation of external biodegradable waste for biogas production is expected in next few years. There are no suitable incineration capacities for sludge incineration. There are some new ideas about incineration of sludge but it is only in the project preparation studies stages. Generally, the attitude (public and “green NGO’s”) towards waste incineration is very negative in the Slovak Republic. Therefore, more dialogue is necessary as well as better understanding of the waste incineration life cycle.

ACKNOWLEDGEMENT

This contribution was supported by the Slovak Research and Development Agency under contracts No. LPP-0019-09.

REFERENCES

1. Hing, C.L., Zenz, D.R. and Kuchenrither, R., “Municipal sewage sludge management— processing, utilization and disposal.” *Water Quality Management Library*, Vol. 4, Technomic Publ., Lancaster 1992.
2. Fyttili D., Zabaniotou A., “Utilization of sewage sludge in EU application of old and new methods—A review.” *Renewable and Sustainable Energy Reviews* 12, 2008, pp. 116–140.
3. Bischofsberger W., Dichtl N., Rosenwinkel K.H. 2005. *Anaerobtechnik*. Springer Berlin.
4. Ministry of Environment of the Slovak Republic: State of the Environment Report of the Slovak Republic 2011, Bratislava, 2012.
5. Commission of European Communities. Council Directive 99/31/EC of 26 April 1999 on the landfill of waste.
6. Commission of European Communities. Council Directive 86/278/EEC of 4 July 1986 on the protection of the environment, and in particular of the soil, when sewage sludge is used in agriculture.
7. Chudoba P., Rosenbergová R., Beneš O., “Benchmarking as a tool for optimisation of sludge management on large WWTPs.” *Proc. from Conference Wastewater 2010*, Štrbské Pleso, 20.-22.10.2010, pp.7–14 (in Czech).
8. Speece R.E., “A survey of municipal anaerobic sludge digesters and diagnostic activity assays.” *Wat.Res.*, 22(3), 1988, pp. 365–372.
9. Appels L., Baeyens J., Degréve J., Dewil R. “Principles and potential of the anaerobic digestion of waste-activated sludge.” *Prog. in Energy and Combustion Science* 34, 2008, pp.755–781.
10. Jeníček P., Bartáček J., Kutil J., Zábranská J., Dohanyos M. “Potentials and limits of anaerobic digestion of sewage sludge: energy self-sufficient municipal wastewater treatment plant.” *Water Sci.Techn.* 66(6), 2012, pp. 1277–1281.

Present and Future Sewage Sludge Treatment in Hungary and its Energetic Utilisation

FERENC ZSABOKORSZKY*

Research and Development Director; ENQUA Kft, Budapest, Hungary

ABSTRACT: Average communal water consumption fell below 100 L/person/day in Hungary. There are 16 sewage treatment plants in Hungary implementing biogas generation with anaerobic treatment. Eleven of these use it to generate electricity. Generating capacity is approximately 9.2 MW. It was inescapable that thermal utilisation of sewage sludge receive a bigger role opposite recultivation in the future. The proportion of agricultural utilisation will not decrease. Price levels of sludge utilisation attain or exceed expenses in Germany without energetic utilisation of sludge.

INTRODUCTION

DISPOSAL and utilisation of sludge generated by wastewater treatment causes many problems in Hungary. The National Wastewater Drainage and Treatment Programme which started in the wake of political transition and accession to the EU is expected to reach completion by 2015. A direct consequence of the programme is a steady increase in sludge generation as new wastewater treatment plants come into operation.

At the same time there is a downward trend in the amount of water supplied in Hungary as seen in other advanced countries. This is the joint result of several factors: economic crisis, falling industrial production, increase in water and drainage charges, and greater environmental awareness. Average communal water consumption fell below 100 L/person/day in Hungary by the end of the first decade of the twenty-first century.

Quality of municipal wastewater depends on the local structure of habitation, degree of industrialisation, and consumption habits. This, together with variations in wastewater and sludge treatment, leads to differences in quality of sewage sludge generated at different sites. There are 678 working plants with capacities ranging from 300 to 260,000 m³/day. Small-capacity sites form the majority.

Four hundred currently operating water utilities manage wastewater drainage greater than 400 million m³ annually. Annual quantity of resulting sludge assuming an average of 25–30% dry matter was 700,000

t/year in 2010. Since the opening of the Budapest Central Wastewater Treatment Plant in 2011 this figure has increased to 900,000 tonnes [1].

CURRENT POSITION OF WASTEWATER SLUDGE UTILISATION

There is a highly varied pattern of wastewater sludge utilisation and disposal in Hungary. This is because the country does not have a sludge disposal and utilisation strategy tailored to local conditions and economic resources. As a result, we see spontaneous emergence of various solutions which do not take account for economic efficiency or future needs.

The fertile land of Hungary is excellently suited to agricultural production. After taking account of disqualifying factors, the country is estimated to have 3 million hectares of land suited for reception of wastewater sludge. There is a further 4 million hectares of agricultural land suited for wastewater compost use. This is approximately one third of the land area of the country.

Another positive factor is that sludge generated by Hungary's sewage works is of high quality and conforms to EU agricultural application criteria [2].

AGRICULTURAL UTILISATION

Direct Agricultural Utilisation of Sludge

Only treated sludge may be applied to the land for which a licence is issued if the landowner consents. The simplest form of sludge treatment is storage for at least six months either thickened at 2–3% dry mat-

*Author to whom correspondence should be addressed.
E-mail: zsabo.ferenc@enqua.hu

Table 1. Distribution of Wastewater Treatment Plants in Hungary by Size of Equivalent Inhabitants.

Equivalent Inhabitant	Number of Plants	Proportion %
< 2000	138	20.4
2001–20,000	341	50.3
20,001–50,000	152	22.4
50,001–100,000	21	3.1
>100,000 p.e.	26	3.8
Total	678	100.0

ter or dewatered at 15–25% dry matter in a watertight reservoir or tank.

This is frequently the method chosen at small-capacity sewage works. Typically, sludge is transported to larger sites with digesters and appropriate utilisation and dewatering capacity. This arrangement has been in operation in the Budapest area since the building of municipal digesters.

Diluted sludge without dewatering is injected directly into the soil. This eliminates the costs of dewatering the sludge and working it into the soil. Its disadvantages are the high cost of transport and the high water content of the sludge. Because of higher resulting from recent changes in fuel prices and ownership structure (reprivatisation), less and less sludge is being used this way.

Costs of disposal are between € 288 and 435 per tonne-dry matter. This is the cheapest mode of agricultural application and all sewage sludge used in this way (154,000 m³/year) is applied to arable land to supply nutrients for crops. The strict framework of legal regulation specifies the quantity of sludge which may be applied without differentiating between soil types.

Sewage sludge compost still does not have realistic market price as a source of plant nutrients, and this impedes its use.

Overall share of sludge disposal methods in Hungary 2012

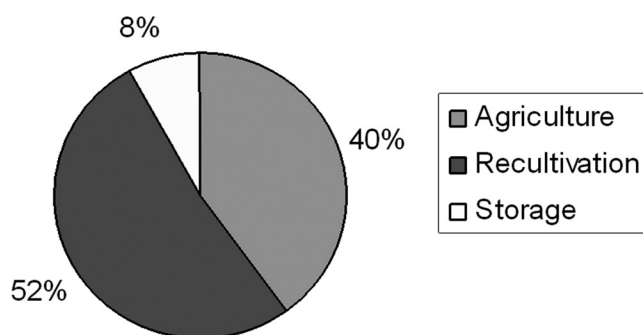


Figure 2. Wastewater sludge disposal at 650 sewage plants, 205,000 t Dm/year in Hungary 2012.

Some landowners are not motivated to use wastewater sludge, and although it is organic fertiliser, there is considerable prejudice against it. This is also a rising trend in other EU countries. Experience in Austria, Germany and Switzerland in recent years indicates the reduction of agricultural application or has acted to reinforce a complete ban.

Composting and Agricultural Use of Wastewater Sludge

Composting of sludge is common in large-capacity wastewater works. The most economic arrangement is to set up a composting facility on site to avoid transport costs. The main problems here are in subsequent use, but it is a good utilisation procedure if there is a suitable agricultural application.

Composting is used for 40% of the sludge produced each year. However, if there are no buyers for the compost the operator has to deposit it or send it for recultivation further adding to costs.

Sludge is the end product of wastewater treatment and contains valuable nutrients, making proper use of it is essential. If energetic utilisation is not possible due to the high capital costs, or insufficient quantities, then composting is to be preferred. It could be particularly useful where direct agricultural application is not possible. Its high phosphorous content in particular makes agricultural application preferable to recultivation. The costs of disposal are between € 250 and 350 per tonne-dry matter. There could be a discussion here of the P utilisation in agriculture versus chemical extraction from sludge, wastewater, or ash

Use of Sludge for Recultivation

This is a widespread application for sludge in Hungary. It essentially involves use as “quasi compost” for covering red sludge and power plant slag storage reservoirs (slurry ponds). The statistics do not reflect the use of this method because they incorporate it under composting. It accounts for 52% of all sludge annually. The disadvantage of this method is the cost of transport for wastewater works remote in relationship to the recultivation area.

The new Budapest Central Wastewater Treatment Plant currently disposes of its sludge at such sites. This alone involves approximately 150,000 tonnes of 28–30% dry matter content per year. Average disposal cost varies depending on distance from € 190 to € 550 per tonne-dry matter. Recultivation should use less

Table 2. Digester Characteristics for Wastewater Plants.

City/Plant	Volume of Digester (m ³)	Gas Production (m ³ /d)	Method of Utilisation
Budapest Észak	2 x 12,000	27,500	Electric power generation to cover the energy requir. of the plant
Budapest Dél	4 x 2,600 és 1 x 2000	27,000	Electric power generation to cover the energy requir. of the plant
Budapest Központi/Main	3 x 5800	23,000	Electric power generation to cover the energy requir. of the plant
Debrecen	2 x 4,500	6,500	Electric power generation to cover the energy requir. of the plant
Kecskemét	1 x 2460, 2 db. 1350	3,000	Electric power generation to cover the energy requir. of the plant
Szeged	2 x 4000	4,000	Electric power generation to cover the energy requir. of the plant
Veszprém	1 x 1000, 1 x 1500	2,500–3,300	Electric power generation to cover the energy requir. of the plant
Sopron	2 x 2,200	2,500	Electric power generation to cover the energy requir. of the plant
Szombathely	2 x 2,500	3,000	Electric power generation to cover the energy requir. of the plant
Zalaegerszeg	2 x 1,540	1,000–1,200	Electric power generation to cover the energy requir. of the plant and CNG for transport
Győr	2 x 3,750	6,000~	Electric power generation to cover the energy requir. of the plant
Ósszesen			107,500
Kapuvár			under construction

valuable material, because the phosphorous content completely drops out of the cycle of use.

Sludge Storage on the Treatment Plant Site

Storage of wastewater sludge in isolated reservoirs (“cold digesters”) occurred on the treatment plant site and serves only to postpone final utilisation. Some 8% of total sludge is put into storage. This material is not being used at all at present, and will only assume a value in future.

Costs of deposition are somewhat higher than agricultural application and lower than recultivation, but this process unfortunately also entails waste. Costs of storage vary between € 50 to € 130 per tonne-dry matter.

ENERGETIC UTILISATION

Biogas generation is an energetic utilisation in contrast with statistical classifications which include this method as a stabilisation procedure within sludge treatment. I will deal only with sludges where biogas is used to generate heat or electric power. The most widespread use of biogas is to reduce the energy costs of wastewater plants. Plants which receive sludge from other sites or waste of high organic content are self-supporting in energy. Budapest No. 2 Wastewater Treatment Plant is one of these, and the Central Plant is 50% self-supporting. Exhaustion of traditional energy sources, the rise and continual fluctuation of oil prices, and worsening environmental problems have forced every country in the world to face the issue of renewable energy.

In order to increase its EU renewable energy quota, Hungary will have to use energy content from sludge wherever possible. After extracting energy from sludge by fermentation the stabilised sludge may be used to replace soil nutrients. This is the approach which has made greatest inroads in sludge treatment in the past 20 years. Extracting energy from sewage sludge requires considerable capital investment.

Anaerobic treatment is one of the most environmentally efficient technologies. Neither does it restrict re-use of phosphorous unlike combustion in coal power plants or use in cement factories. The process also eliminates methane emissions from sludge and reduces sludge quantity. The process may generate several different products: biogas, electric power, heating hot water, propellant, and organic fertiliser. The greatest barrier to using energy from sewage sludge is the relatively high initial capital cost, not using wastewater sludge is equivalent to squandering resources. It is also possible to say that wastewater sludge is equivalent to grey gold (e.g., Biogas development for the City of Zalaegerszeg as fuel for municipal public transport).

Establishing biogas plants based on communal wastewater sludge is primarily a task for central- and local-government sectors. Gas or electric power generation may be used to cover energy requirements for the plant itself.

ENERGETIC UTILISATION IN HUNGARY IN THE EUROPEAN PERSPECTIVE

No sludge is incinerated or used in cement works in Hungary at the present time. This form of use has

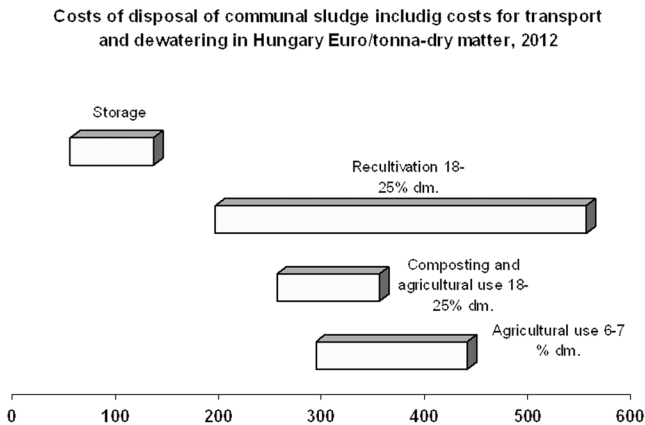


Figure 2. Disposal costs in Hungary.

received no government support in recent years and in fact has been out of favour. There are tests, or experimental operations, in several plants but for various reasons they have not been expanded. By comparison, thermal utilisation in Germany has increased from 9% to 40% of the total in the past 20 years. The proportion of thermal utilisation attained 53% and recultivation decreased to half this at 16% in Germany. The proportion of agricultural utilisation did not change at 30% [3].

Causes may be traced to the National Wastewater Programme which was launched following the country's EU accession in 2004 and concerned with developing municipal drainage and sewage treatment. No attention or resources were devoted to the possibility of municipalities cooperating to build joint thermal utilisation plants. Incineration of small quantities of sludge would not be economic. A potential opportunity was construction of the new Budapest Central Wastewater Treatment Plant, Central Europe's largest EU-supported environmental project with a nominal capacity of 350,000 m³ per day. Digesters were built but without thermal utilisation.

Comparison of Disposal Costs

Comparing disposal expenses a surprising result

is observed. Price levels attain or exceed expenses in Germany without energetic utilisation of sludge. The highest mono-incineration costs don't exceed € 400 per tonne-dry matter in Germany at the same time the cost of recultivation is more than € 550 per tonne-dry matter in Hungary. Regarding comparison of disposal expenses, data from the Federal environment protection office was used [3].

SUMMARY

Proportions of agricultural utilisation will not decrease. It is the experience in EU countries that tightening regulations stimulate increasing energetic utilisation of sewage sludge. The essence of EU energy policy in pursuit of sustainable development is to make renewable energy competitive.

There are 16 sewage treatment plants in Hungary which implement biogas generation with anaerobic treatment and 11 of these use it to generate electricity. They use electricity to supply their own needs. Generating capacity is approximately 9.2 MW. The price level attains or exceeds expenses in Germany without energetic utilisation of sludge.

The new Hungarian National Waste Management Agency now supervises collection, transport, and utilisation of domestic waste. Considering that wastewater sludge is a secondary raw material of no less strategic importance than domestic waste there seems to be a good argument of its utilisation to be put under supervision of new Water Utilities Authority. The Authority is responsible for setting charges and overseeing investments. It would be necessary to carry out an analysis of present means of utilisation set against developments in Europe to make a proposal for further action.

REFERENCES

1. Ölős G.-Oláh J.-Palkó Gy. : Rothasztás–MAVÍZ 2010 (p.1015–1067)
2. Fikérmé, Sulcz Á.: A rothasztott szennyvíziszap hasznosítása. Hulladéksors, No. 5., 2011.
3. Wiechmann B. *et al.*: Klärschlammensorgung in der Bundesrepublik Deutschland. Umweltbundesamt (UBA), 2012.

Modeling of Wastewater Sludge Drying with Determination of Diffusivity Moisture

L. BENNAMOUN^{1,*}, L. FRAIKIN², T. SALMON², M. CRINE² and A. LÉONARD²

¹Department of Mechanical Engineering, University of New Brunswick, Fredericton, Canada

²Laboratory of Chemical Engineering, University of Liège, Belgium

ABSTRACT: Convective drying of two different wastewater sludges is investigated. Experiments are realized in a micro-dryer, for air temperatures of 80°C, 140°C and 200°C, the air velocity and humidity remaining the same. The product drying kinetics presents, for all studied cases, three main phases, which are: adaptation phase, constant drying rate phase and falling drying rate. A comparison between the graphical representation of the drying curve and the analytical solution of diffusion equation allows determination of the diffusion coefficient. The value of this coefficient depends on the origin of the wastewater sludge and the operating temperatures. Physical changes such as shrinkage are introduced into the mathematical model.

INTRODUCTION

NOVEL solutions are required due to world population's increasing demand for water and the non-availability of this crucial resource in some regions. A novel technological solution is development of wastewater treatment plants (WWTP). However, this facility of interest is at the origin of sludge production which has to be managed to be valorized at its best organic and mineral content or energy content. Among preferable solutions, incineration and use in agriculture are possibilities, with relative importance depending on location.

Drying is a non-avoidable step for sludge transformation. It permits decrease of handling costs, transport, and storage by reducing sludge mass and volume, or its use as a combustible due to increased calorific value. Several scientific works, with the help of mathematical modeling and simulation, are directed to know more about fundamental aspects of wastewater sludge behaviour during drying and as well as understating parameter influence during this process. It allows for optimum results for better control.

Léonard *et al.* [1] studied influence of operating conditions for temperature, humidity, and superficial velocity of air on the behaviour of several wastewater sludge's during convective drying and after mechani-

cal dewatering. A clear dominance is registered for air temperature. Determination of coefficients of heat and mass transfer and water evaporation capacity are also performed by the authors using drying kinetics results. The origin of the sludge is found as another parameter influencing general behaviour of sludge during convective drying [2]. Shrinkage and cracks are two phenomena that appear during convective drying of wastewater sludge and evidently observed using X-ray microtomography [3–5]. The non-introduction of these phenomena during modeling and simulation [6–7] may lead to an over-estimation of heat and mass parameters as found by Rahman and Kumar [8] for food application.

In a different manner, drying wastewater sludge is explored using indirect agitated techniques. The product passes through three phases from respectively wetted to dried product that are pasty, lumpy, and granular [9,10]. During application of this methodical influence of pressure, heating temperature, stirrer speed, and particle size results are reviewed. Modeling and simulation permit an observation of variation for several drying parameters, such as heat transfer coefficient and penetration resistance [10–12] for the product behaviour.

Experimental results of convective drying for two different types of wastewater sludge are presented in this paper. The work is reinforced with modeling and simulation, allowing determination of the sludge diffusion coefficient. Variations in physical changes of the product represented essentially by shrinkage are introduced in the model.

*Author to whom correspondence should be addressed.
E-mail: Lyes.Bennamoun@unb.ca

MATERIALS AND METHODS

Sample Preparation

This study focuses on two very different sludges: an activated sludge (AS) from a WWTP of Grosses Battes, Liège and a thermolyzed and digested sludge (TDS) from a WWTP of Bruxelles-Nord, Brussels. Water to be purified undergoes a primary treatment, an anaerobic phase, and an alternating aerobic/anoxic phase to produce AS. Finally, phosphate is precipitated by ion chloride and biomass and in excess is dewatered using a belt filter. TDS undergoes the same treatments except dehydration is carried out by centrifugation. Afterward, TDS is subject to a temperature of 160°C and a pressure of 6 bars for 30 minutes. The sludge is then flashed and digested to produce biogas.

It is important to note that for (AS) the sludge is collected after the mechanical dewatering step. The sample initial dry matter content was close to 14.5%. Sludge is stored in tightly closed jar before drying at a temperature of 4°C.

Instrumentation and Measurements

Before drying, sludge samples are extruded in cylindrical shape (diameter = height = 15 mm). Drying experiments are carried out in a discontinuous pilot-scale dryer (Figure 1) reproducing most of the operating conditions prevailing in a full-scale continuous belt dryer. Ambient air is heated up to the required temperature by an electrical heating device and may be humidified by adding steam.

Three operating conditions are controlled throughout the drying process: temperature (50–200°C), superficial velocity (1–3 m/s), and air humidity (0.005–0.5

Table 1. Semi-theoretical Fitted Models.

Number	Model Equation	Name of the Model
1	$X^* = \exp(-k \cdot t)$	Newton
2	$X^* = \exp(-k \cdot t^n)$	Page
3	$X^* = a + b \cdot t + c \cdot t^2 + d \cdot t^3 + e \cdot t^4$	4th degree polynomial
4	$X^* = a \cdot \exp(-k \cdot t)$	Henderson and Pabis

$\text{kg}_{\text{water}}/\text{kg}_{\text{dry air}}$). Air humidity is checked on-line with a cooled mirror dew point hygrometer. Initial mass of the sample is 2.5 g and dynamics of weight over time is followed on-line via continuous weighing. Data points are recorded every 30 s. The surface change and product surface temperature are registered using the surface camera and infrared pyrometer, respectively.

MATHEMATICAL MODELING

The mathematical modeling treatment is divided into two parts. First, experimental results are fitted and semi-theoretical models are proposed (Table 1). The analytical solution of the equation of diffusion represented by Fick's second law was used as a second approach. Comparison between the two results permits determination of the diffusion coefficient.

Semi-Theoretical Models

Experimental drying curves are fitted using Curve-Expert software. The best models are those presenting the best correlation coefficient (r) and lowest value of standard error (χ^2). Results show that the 4th degree model presents better results. However, this model has no-real physical meaning like the Page model with a correction factor (n). The Henderson and Pabis model presents good fitting results and is considered as be-

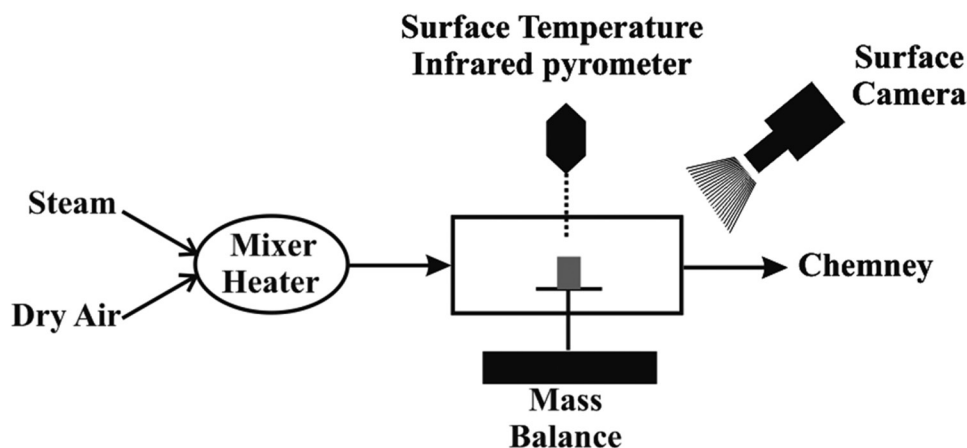


Figure 1. Simplified schema for a convective drying system.

Table 2. Fitting Results of the Different Semi-theoretical Models for Sludge (AS).

Number	Temperature 80°C			Temperature 140°C			Temperature 200°C		
	Parameters	(r)	(χ ²)	Parameters	(r)	(χ ²)	Parameters	(r)	(χ ²)
1	k = 0.02932	0.99647	0.02337	k = 0.07450	0.99529	0.02754	k = 0.08077	0.98904	0.04482
2	k = 0.01769 n = 1.13480	0.99908	0.01198	k = 0.04435 n = 1.18455	0.99953	0.00871	k = 0.03567 n = 1.30239	0.99927	0.01165
3	a = 1.01599 b = -0.02748 c = 0.00033 d = -2.13842 × 10 ⁻⁶ e = 5.96414 × 10 ⁻⁹	0.99997	0.00221	a = 1.01062 b = -0.06395 c = 0.00155 d = -1.77418 × 10 ⁻⁵ e = -8.65103 × 10 ⁻⁸	0.99989	0.00434	a = 1.02349 b = -0.06399 c = 0.00108 d = 3.48503 × 10 ⁻⁶ e = -1.68941 × 10 ⁻⁷	0.99987	0.00508
4	a = 1.05158 k = 0.03077	0.99767	0.01901	a = 1.06258 k = 0.07891	0.99702	0.02204	a = 1.10004 k = 0.08836	0.99368	0.03429

ing closer to the diffusion approach. Fitting results of sludge (AS) are presented in Table 2.

Comparison between experimental results and theoretical results based on fitting results for sludge or AS are displayed in Figure 2. The model displays great agreement with a small divergence at high temperatures. TDS sludge has displayed the same general affinity.

Diffusion Model

Water distribution inside the product is described by Fick’s law. For the unsteady state and one dimensional case, the equation of diffusion is written in the following form:

$$\frac{\partial X}{\partial t} = D_{eff} \left(\frac{1}{y^n} \right) \left(\frac{\partial}{\partial y} \right) \left[y^n \frac{\partial X(y,t)}{\partial y} \right] \quad (1)$$

Where *n* takes the value of “0” for a plate, “1” for a cylinder, and “2” for a sphere.

Considering convective conditions, Equation (1) is solved by assuming:

- Distribution of initial moisture is uniform thought the solid.
- Surface of the solid is at equilibrium with air for a considered time.

Crank [14] proposed an analytical solution for each case studied employing multiple dimensional studies with various conditions applied. In the process of assessing complexity of the proposed solutions, users may have a tendency to simplify the treated problem by considering an infinite one-dimensional case. This approximation does not always provide correct results as confirmed by Rahman and Kumar [8]. For this study the sample has a cylindrical shape with an equal diameter and a height of 15 mm. It is evident that the cylinder cannot be considered infinite.

The analytical solution of the equation of diffusion for a finite cylindrical shape was also proposed by Crank [13] and used by Usub *et al.* [14] and McMinn and Magee [15]. It takes the following form:

$$X^* = \frac{X}{X_0} = \frac{8r^2}{l^2} \sum_{i=1}^{\infty} \sum_{j=1}^{\infty} \frac{1}{\lambda_i^2 \beta_j^2} \exp \left(-(\lambda_i^2 \beta_j^2) \frac{D_{eff} t}{r^2} \right) \quad (2)$$

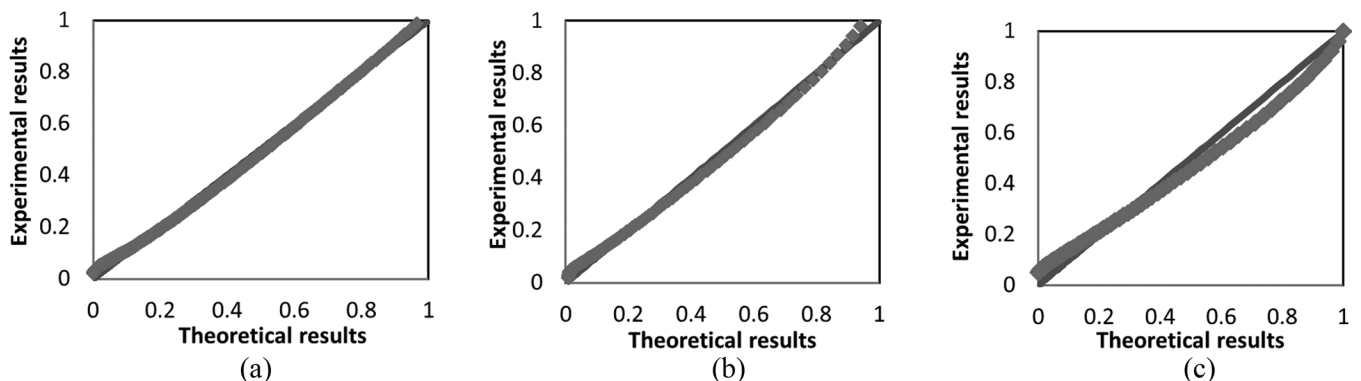


Figure 2. Comparison between experimental results and Henderson and Pabis model: (a) 80°C, (b) 140°C, and (c) 200°C.

With:

$$\beta_j = \frac{(2j-1)\pi r}{2l} \quad (3)$$

λ_i is the root of the Bessel function.

For long drying times ($X^* < 0.6$) only the first term of the series solution is taken into account, which gives:

$$X^* = \frac{32}{\lambda_1^2 \pi^2} \exp\left(-(\lambda_1^2 + \beta_j^2) \frac{D_{eff} t}{r^2}\right) \quad (4)$$

The plot of the experimental results in term of $\ln(X^*)$ versus drying time gives a straight line with a slope:

$$slope = (5.7831 + \beta_1^2) \frac{D_{eff}}{r^2} \quad (5)$$

Introduction of Shrinkage

Shrinkage in this study is introduced by calculation of instant variations of physical sample characteristics so mass of product may be presented as function of moisture content as written in Equation (6):

$$m = (X + 1)m_{dry} \quad (6)$$

The surface and the volume of the particle take the following form, respectively:

$$S(X) = 2\pi R(X)((R(X) + L(X))) \quad (7)$$

$$V(X) = \pi R^2(X)L(X) \quad (8)$$

Dimensional variations are then easily calculated. Additionally, in a previous study, it was found that these variations happen in an isotropic manner [5]. Consequently, variations of product density, shrinkage (Equation 9), and characteristic dimension (Equation 10) may be followed.

$$Shrinkage = 1 - V(X)/V_0 \quad (9)$$

$$\delta(X) = \left(\frac{2}{L(X)} + \frac{2}{R(X)}\right)^{-1} \quad (10)$$

Figure 3 displays a decrease in volume with a product moisture content decrease. This decrease takes a linear form and depends on sludge type. Therefore, as the final normalized volume of TDS sludge attains 0.4 it is around only 0.55 for AS sludge.

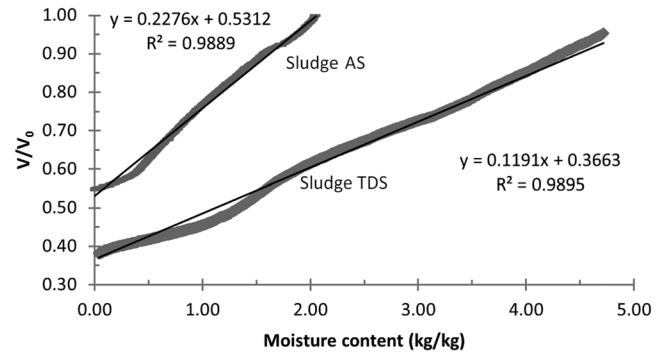


Figure 3. Experimental results for volume decrease for AS and TDS during drying at 80°C.

RESULTS AND DISCUSSION

Experiments are realized under the same constant operating conditions for the two sludges. These conditions are displayed in Table 3.

AS has an initial moisture near 2 kg/kg (dry basis) and is around 5 kg/kg for the TDS sludge. Precedent studies have shown that convective sludge drying passes through three main phases: adaptation phase, constant drying rate phase, and falling drying rate phase [1–2,6]. Additional studies confirm there is an absence of the constant drying rate phase when utilizing evaporation rate ($\text{kg}\cdot\text{s}^{-1}$) vs. moisture content without introducing surface variations [7]. As shrinkage occurs with an important reduction of volume reaching more than 60% (Figure 3), it is more adequate to represent the evaporation rate per surface unit. Figure 4 representing results for the two sludges of interest displays a short first phase of adaptation, a short constant drying rate period, and a long falling drying rate phase. Using another perspective, it gives information about influence of operating conditions, and notes particular air temperature as increasing temperature increases evaporation flux rate. Sludge origin is also upsetting flux evaporation and it is evident to find that TDS with more initial moisture content has more important evaporated quantities with higher maximal values of flux than AS.

Figure 5 illustrates the evolution of surface temperature obtained by infrared pyrometer at 200°C air temperature. The figure shows that required energy

Table 3. Applied Operating Conditions.

Temperature (°C)	Velocity ($\text{m}\cdot\text{s}^{-1}$)	Humidity ($\text{kg}_{\text{water}}/\text{kg}_{\text{dry air}}$)
200	1	0.005
140	2	0.05
80	1	0.005

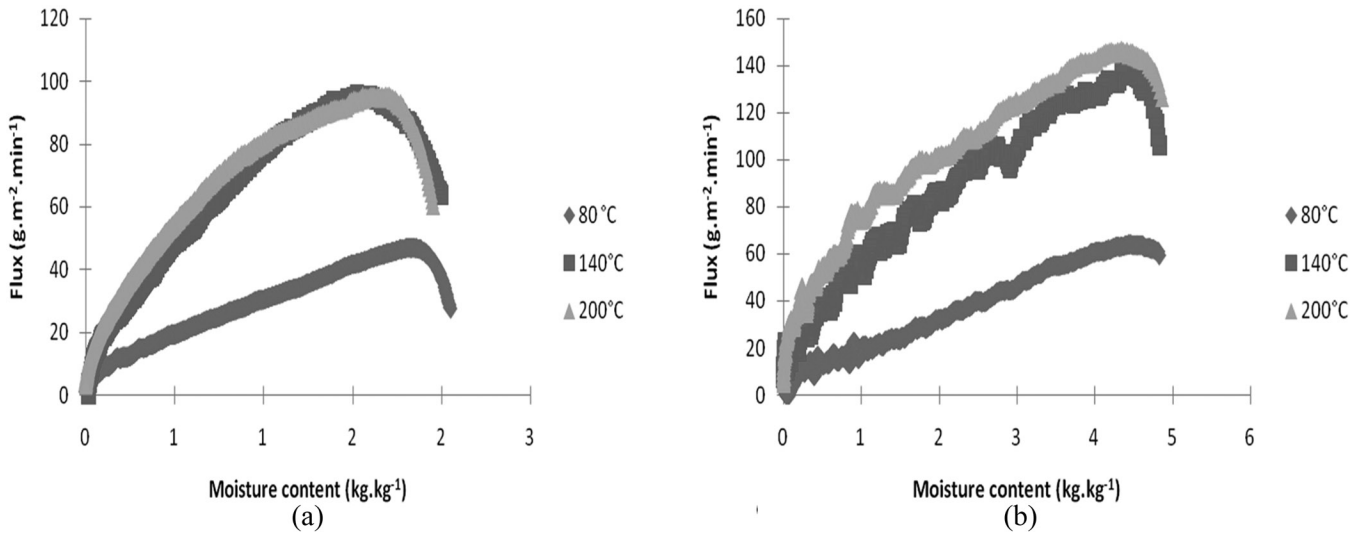


Figure 4. Illustration of evaporation flux vs. moisture content, (a) AS and (b) TDS.

for all phases does not serve only to evaporate product moisture, but also to increase product temperature. The figure displays a continuous increase of product temperature with a degree in moisture content (i.e., end of the drying process). Furthermore, origin of sludge influences temperature increase as seen in Figure 5. Product temperature of AS sludge that contains less water is more important than TDS sludge.

Determination of Diffusion Coefficient

The diffusion coefficient is obtained by comparing fitting results and slope obtained by graphical representation of $\ln(X^*)$ versus time. However, a parametric study done by Rahman and Kumar [8] showed overes-

timization of value for the diffusion coefficient by neglecting shrinkage phenomena or by considering the sample having an infinite geometry. Consequently, in this study the sample is simulated with a finite geometry and the solution for the diffusion equation is represented by Equations (4) and (5) with a recalculation of sample physical parameters for every time step.

The value of the diffusion coefficient depends on origin of wastewater sludge and operating temperatures. It has an average mean value of $4.46 \cdot 10^{-9} \text{ m}^2 \cdot \text{s}^{-1}$ for AS sludge and decreases to $3.62 \cdot 10^{-9} \text{ m}^2 \cdot \text{s}^{-1}$ for TDS sludge at the same temperature of 80°C. These coefficients increase to a value of $13.47 \cdot 10^{-9} \text{ m}^2 \cdot \text{s}^{-1}$ for the AS sludge and $9.67 \cdot 10^{-9} \text{ m}^2 \cdot \text{s}^{-1}$ for the TDS sludge at 200°C.

Figure 6 presents the variation of the mean value of diffusion coefficient with air temperature. It is written in the Arrhenius relation and the constant D_0 and Activation energy (E) are deduced. Results for both sludges are provided in Table 4.

CONCLUSIONS

Results have suggested wastewater sludge is affected by applied operating conditions and in particular the air temperature and also by sludge origin. Comparison between AS and TDS drying results display that

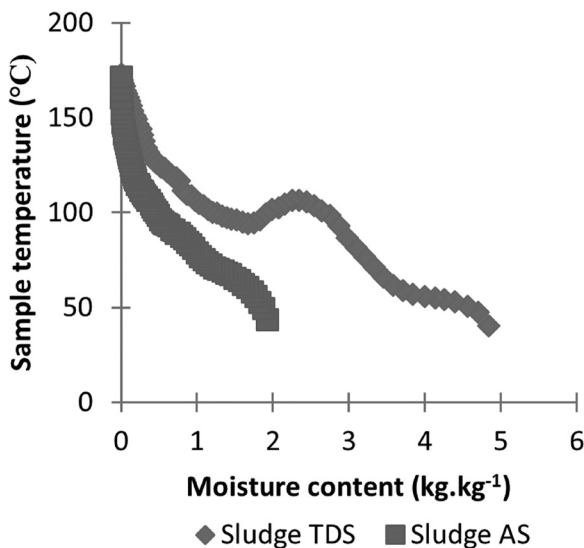


Figure 5. Evolution of surface product temperature vs. moisture content.

Table 4. Determination of Diffusion Coefficient Parameters.

Sludge Type	$D_0 \text{ (m}^2 \cdot \text{s}^{-1}\text{)}$	$E \text{ (kJ} \cdot \text{mol}^{-1}\text{)}$
As	4.5181×10^{-7}	13.21
TDS	2.3120×10^{-7}	11.97

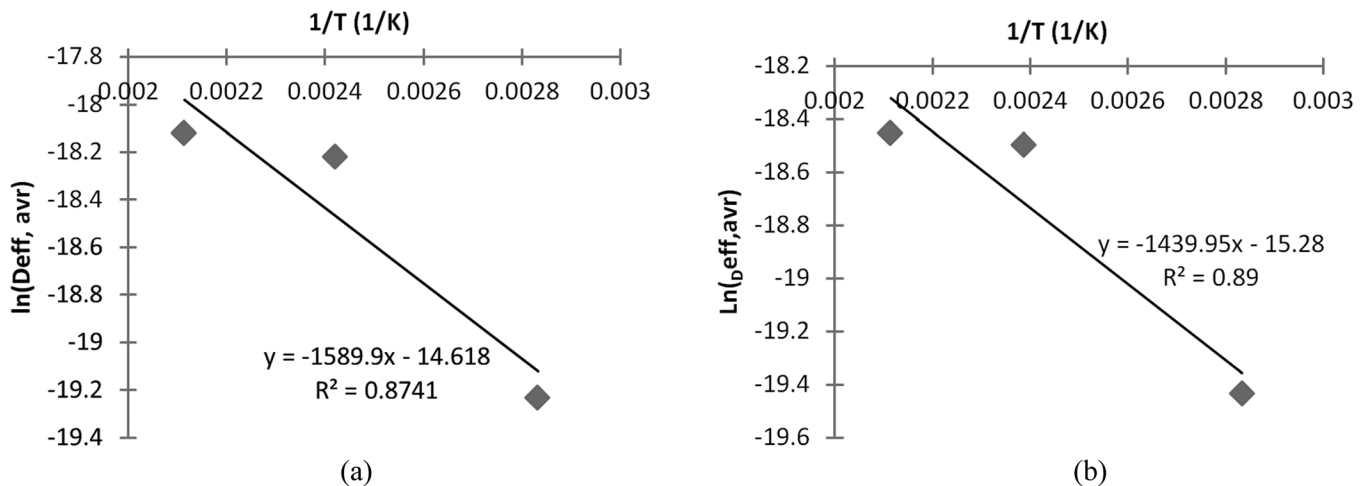


Figure 6. Influence of air temperature on mean value of diffusion coefficient, (a) AS and (b) TDS.

TDS attains maximal values of evaporated flux with a lesser diffusion coefficient. An increase of product temperature was more important for AS than for TDS. Diffusion coefficients were less important than those obtained by Reyes *et al.* [6] and higher than those obtained by Léonard *et al.* [16]. To confirm importance of considering shrinkage and finite geometry on values of the diffusion coefficient, a calculation without these parameters is made. Similar to remarks obtained by Rahman and Kumar [8], results show that not considering the finite shape of the sample or not taking into account shrinkage phenomena gives an over estimation of the diffusion coefficient (e.g., diffusion coefficient has doubled its value when shrinkage is not considered with $7.42 \cdot 10^{-9} \text{ m}^2 \cdot \text{s}^{-1}$ at 80°C and $22.87 \times 10^{-9} \text{ m}^2 \cdot \text{s}^{-1}$ at 200°C for TDS).

ACKNOWLEDGMENTS

L. Bennamoun and L. Fraikin are thankful to the FRS-FNRS for their postdoctoral fellow positions (FRFC projects 2.4596.10 and 2.4596.12).

REFERENCES

- Léonard, A., Blacher, S., Marchot, P., Pirard, J. P., Crine, M., "Convective drying of wastewater sludges: influence of air temperature, superficial velocity, and humidity on the kinetics", *Drying Technology*, Vol. 23, No. 8, 2005, pp. 1–13.
- Léonard, A., Vandevenne, P., Salmon, T., Marchot, P., Crine, M., "Wastewater sludge convective drying: Influence of sludge origin", *Environmental Technology*, Vol. 25, No. 9, 2004, pp. 1051–1057.
- Léonard, A., Blacher, S., Pirard, R., Marchot, P., Crine, M., "Multiscale texture characterization of wastewater sludges dried in a convective rig", *Drying Technology*, Vol. 21, No. 8, 2003, pp. 1507–1526.
- Léonard, A., Blacher, S., Marchot, P., Crine, M., "Use of X-ray microtomography to follow the convective heat drying of wastewater sludges", *Drying Technology*, Vol. 20, No. 4–5, 2002, pp. 1053–1069.
- Tao, T., Peng, X. F., Lee, D.J., "Thermal drying of wastewater sludge: change in drying area owing to volume shrinkage and crack development", *Drying technology*, Vol. 23, No. 3, 2005, pp. 669–682.
- Reyes, A., Eckholt, M., Troncoso, F., Efmov, G., "Drying kinetics of sludge from a wastewater treatment plant", *Drying technology*, Vol. 22, No. 9, 2004, pp. 2135–2150.
- Font, R., Gomez-Rico, M. F., Fullana, A., "Skin effect in the heat and mass transfer model for sewage sludge drying", *Separation and Purification Technology*, Vol. 77, No. 1, 2011, pp. 146–161.
- Rahman, N., Kumar, S., "Evaluation of moisture diffusion coefficient of cylindrical bodies considering shrinkage during natural convection drying", *International Journal of Food Engineering*, Vol. 7, No. 1, 2011, Article 4.
- Deng, W. Y., Yan, J. H., Li, X. D., Wang, F., Lu, S. Y., Chi, Y., Cen, K. F., "Measurement and simulation of the contact drying of sewage sludge in a Nara-type paddle dryer", *Chemical Engineering Science*, Vol. 64, No. 24, 2009, pp. 5117–5124.
- Ferrasse, J. H., Arlabosse, P., Lecomte, D., "Heat, momentum, and mass transfer measurements in indirect agitated sludge dryer", *Drying Technology*, Vol. 20, No. 4–5, 2002, pp. 749–769.
- Yan, J. H., Deng, W. Y., Li, X. D., Wang, F., Chi, Y., Lu, S. Y., "Experimental and theoretical study of agitated contact drying sewage sludge under partial vacuum conditions", *Drying Technology*, Vol. 27, No. 6, 2009, pp. 787–796.
- Arlabosse, P., Chitu, T., "Identification of the limiting mechanism in contact drying of agitated sewage sludge", *Drying Technology*, Vol. 25, No. 4, 2007, pp. 557–567.
- Crank, J. 1975. *The mathematics of diffusion*, Oxford, England.
- Usub, T., Lertsatitthakorn, C., Poomsa-ad, N., Wiset, L., Siriamornpun, S., Soponronnarit, S., "Thin layer solar drying characteristics of silkworm pupae", *Food and Bioproducts Processing*, Vol. 88, No. 2–3, 2010, pp. 149–160.
- McMinn, W. A. M., Magee T. R. A., "Principals, methods and applications of the convective drying of foodstuffs", *Food and Bioproducts Processing*, Vol. 77, No. 3, 1999, pp. 175–193.
- Léonard, A., Blacher, S., Marchot, P., Pirard, J. P., Crine, M., "Moisture profiles determination during convective drying using X-ray microtomography", *The Canadian Journal of Chemical Engineering*, Vol. 83, No. 1, 2005, pp. 127–131.

Penetrant Liquid Waste Degradation by Radiocatalysis

JAIME JIMÉNEZ-BECERRIL^{1,*}, JULIO CÉSAR GONZÁLEZ-JUÁREZ² and ROBERTO CONTRERAS-BUSTOS³

¹Departamento de Química, Instituto Nacional de Investigaciones Nucleares, Apartado Postal 18-1027. México, D.F. 11801 México

²Instituto Tecnológico de Toluca, Av. Instituto Tecnológico S/N, Metepec, Estado de México, México, 52140 México

³Centro de Investigación y Desarrollo Tecnológico en Electroquímica (CIDETEQU), Parque Tecnológico Querétaro Sanfandila, 76703 Pedro Escobedo, Qro., México

ABSTRACT: Penetrant liquids are mixtures of solvents and organic compounds used in industry for non-destructive tests of metallic pieces. However, during the final stage penetrant liquids are wiped with water leaving a large amount of wastewater. Waste disposal methods use an absorbent material and dispose of it in compliance with all local, state, and federal regulations. In this work, radiocatalysis was used as an alternative method for treatment of penetrant liquid waste. Experiments with penetrant liquids in different concentrations were gamma irradiated using a cobalt-60 source. For some samples, TiO₂ was added as a catalyst and then gamma irradiated. UV spectrophotometry and chemical oxygen demand (COD) were used to measure residual penetrant liquid. Gamma-induced degradation of the penetrant liquid was found to improve when the catalyst was added and the amount depended on the penetrant liquid concentration. This study is motivated for potential use of irradiation of semiconductors as catalysts and as a means of mineralization and purification of organic pollutants in aqueous media.

INTRODUCTION

LIQUID penetrant testing also known as dye penetrant testing is used to confirm presence of a crack or flaw in metallic pieces. The basic stages of liquid penetrant inspection are as follows. The surface to be inspected is cleaned thoroughly to remove all traces of dirt and grease. Then a brightly colored or fluorescent liquid is applied liberally to the component's surface and allowed to penetrate any surface-breaking cracks or cavities. The liquid is allowed to soak into the material's surface for about 20 minutes. After this soaking, the excess liquid penetrant is wiped from the surface and a developer is applied. The developer is usually a dry white powder that draws the penetrant out of any cracks by reverse capillary action to produce colored indications on the surface. These indications are broader than the actual flaw, and they are, therefore, more easily visible [1].

This water-washable, inspection penetrate process is used extensively for the non-destructive testing and inspection of critical aircraft parts for potential failure flaws. The hazardous properties to consider when

choosing or designing any system are the liquid's flash point and toxicity [2].

Penetrants may contain a blend of aromatic and aliphatic hydrocarbon solvent(s), refined mineral oil(s), dye, surface active agent(s), alcohol(s), and hydrocarbon propellant(s). The ingredients of the developer may include 2-propanol, 2-propanone, isobutane, and talc. The surface penetrant removed from test parts becomes mixed with the washing water and is discarded into the nearest sewage or water disposal system. In some cases, efforts are made to extract the penetrant from the washing water to minimize pollution in wastewater effluents, but this is quite difficult in the case of readily soluble or easily emulsified penetrants. Sometimes, hazardous waste generated on site is stored pending collection by approved waste contractors [3]. Main components of penetrants in their individual form are not considered highly hazardous materials, but have a potential risk for occupational and consumer exposure through inhalation and skin contact. However, exposures through inhalation are expected to be high due to the low vapor pressure.

Given the fact that regulations are dynamic and analysis interpretations are not foolproof, there are situations in which the use of environmentally friendlier products will not pass the local requirements, and

*Author to whom correspondence should be addressed.
E-mail: jaime.jimenez@inin.gob.mx

the penetrant process effluent must be treated. This is accomplished most easily at the source of the waste generation rather than after several different waste streams have been combined. A number of methods are available to help meet these regulations: bleach, carbon filtration, ozone treatment, membrane filtration, and removal by an absorbent media [4]. Meas *et al.* [5] determined that by using an electrocoagulator with sacrificial electrodes, chemical oxygen demand (COD) (95%), color (99%), and turbidity (99%) can be reduced when testing fluorescent, penetrated liquid for the non-destructive testing of parts. The water was reused four times.

Heterogeneous radiocatalysis may be considered a viable alternative for the removal of refractory organics. It has several important advantages, such as the complete mineralization or formation of more readily biodegradable intermediates when complex organic compounds are treated, the lack of a need for auxiliary chemicals and residual formation, and the ease of operation and maintenance of the equipment. Research on heterogeneous radiocatalysis provides information on the possibilities and efficiencies encountered in the application of this process for industrial wastewater treatment for the removal of different types of refractory organic compounds.

Although the degradation of penetrant liquid waste can be treated with biological methods, radiolysis and radiocatalysis were examined as a non-conventional treatment system, proposed to remove a complex mixture of industrial organic chemical wastewater containing penetrant liquids.

The radiolysis of pure deaerated liquid water by γ -rays or high energy electron leads to the formation of free radicals (e_{aq}^- , H^\bullet , $\bullet OH$) and molecular species (H_2 , H_2O_2). The yields ($G_{e_{aq}^-}$, G_{H^\bullet} , G_{OH^\bullet} , G_{H_2O} and $G_{H_2O_2}$) representing the number of species of each kind formed by 100 eV of absorbed energy are well established [6].

Hydrogen formation in water radiolysis with suspensions of photocatalyst particles has been studied. Chitose [7] observed that the yield of H_2 was found to be greater for radiolysis in the presence of different catalysts than in pure water [8]. The reported results show that relatively low doses of gamma irradiation have a weak effect on the TiO_2 crystal structure and morphology. No changes were observed in the phase decomposition or the general profile of the X-ray diffraction patterns. The changes in grains size, specific surface area, and crystallite size were insignificant [9-12].

The synergy between gamma radiation, UV radia-

tion or high energy electrons, and the presence of catalyst of photocatalyst leads to the conclusion that the effect of the catalyst enhances the mineralization of the organic compounds [11,13,14].

MATERIAL AND METHODS

Depleted commercial penetrant liquid, after having been used in an industry without further purification or treatment, was used. Depleted commercial penetrant liquid was used without further purification or treatment. The received sample was stored at room temperature in dark conditions and, after seven days, showed three phases: a solid precipitate, a solid that floats, and an aqueous phase. Solids were separated by decantation, and it is possible to apply other processes for treatment. Only the aqueous phase was used in the experiment. The sample was a mixture of different compounds. Generators of residues reported that liquid waste could contain ethylene glycol as an emulsifier, polyethylene glycol ether and isocyclodiphenylphosphate mixed with hydrotreated middle petroleum distillate, and esters and phthalate as a penetrant.

The initial concentration of individual components was unknown. Alcohols and ethers do not absorb light in the environmentally significant range (> 290 nm). Therefore, these compounds should not undergo direct photolysis in the environment and show no hydrolysable groups, meaning they are not susceptible to hydrolysis. The sample, considered a reference, was of high concentration, and dilutions were prepared with a ratio of 1:9, 2:8, and 3:7 penetrant liquid concentrate waste to water. TiO_2 (Degussa P25) was added as a catalyst to the dilutions at a rate of 1 g/L, and suspensions were put in 10-mL glass vials. The gamma irradiation was conducted with a ^{60}Co source in a Transelektro LG-01 gamma irradiator. The principal advantages of such small irradiators are that they are easy to install and operate, and they provide high dose rates and good dose uniformity, which are essential for radiation research. These characteristics are achieved by surrounding the sample with radiation source pencils such that it receives radiation from all directions (cylindrical irradiation chamber with length 14 cm and diameter 10 cm). A functional accumulated dose range of 5 to 15 kGy was applied with a dose rate of 27.9 kGy/h using absolute dosimetric techniques.

After irradiation, TiO_2 particles were removed by filtration with a Millipore membrane of 0.45 μm to provide transparent, non-scattering solutions, suitable for measurements by UV spectrophotometry. Standard

Table 1. UV Absorption Measurements of Penetrant Liquid Dilutions at Different Conditions.

Dilution	UV ₂₅₄ as DOC (mg/L)			
	No Irradiation and No Catalyst	No Irradiation and Catalyst	No Catalyst and Irradiated at 15 kGy	With Catalyst and Irradiated at 15 kGy
1:9	126.5	116.7	58.2	21.2
2:8	230.9	191.4	164.4	155.3
3:7	258.5	244.5	226.0	212.0

method [15] was used for the determination of UV absorption at 254 nm (UVA) in a spectrophotometer (Perkin Elmer UV/VIS lambda 35, nm, 1 cm quartz cell).

COD was measured according to standard procedure using Hach DRB200 equipment. The technique involves boiling 10 mL of the sample at 150°C for 2h in an 8 mol/L H₂SO₄ solution with the introduction of K₂Cr₂O₇ as an oxidizing agent, Ag₂SO₄ as a catalyst, and HgSO₄. The non-reacted CrO₇²⁻ is removed by titration with Fe(NH₄)₂(SO₄)(6H₂O) using a ferroin indicator [16].

RESULTS AND DISCUSSION

According to standard method [14], UV absorbance of fulvic acids was used as a reference in determination of UV-absorbing organic constituents in the samples. Figure 1 shows the UV spectrophotometry of the first

dilution using 1 mL of depleted penetrant liquid waste and 9 mL of water. Figures 1(a) and 1(b) correspond to the samples without irradiation. It was noticed that organic compounds were adsorbed in small amounts by the catalyst. Although UV absorption can be used to detect certain individual organic contaminants after separation (e.g., by HPLC), the method used here is not suitable for detection of trace concentrations of individual chemicals. It is intended to be used to provide an indication of the aggregate concentration of UV-absorbing organic constituents. Several conventional methods could eliminate components of the mixture, but the interest was centered on to the hypothesis that radiolysis and radiocatalysis can work as a degradation method in industrial residual waste. Organic adsorption in the 254 nm region is lower than in the 373 nm region. Transitions $n \rightarrow \pi^*$ are located in the carbonyl group, mainly aldehydes and ketones. Molar absorp-

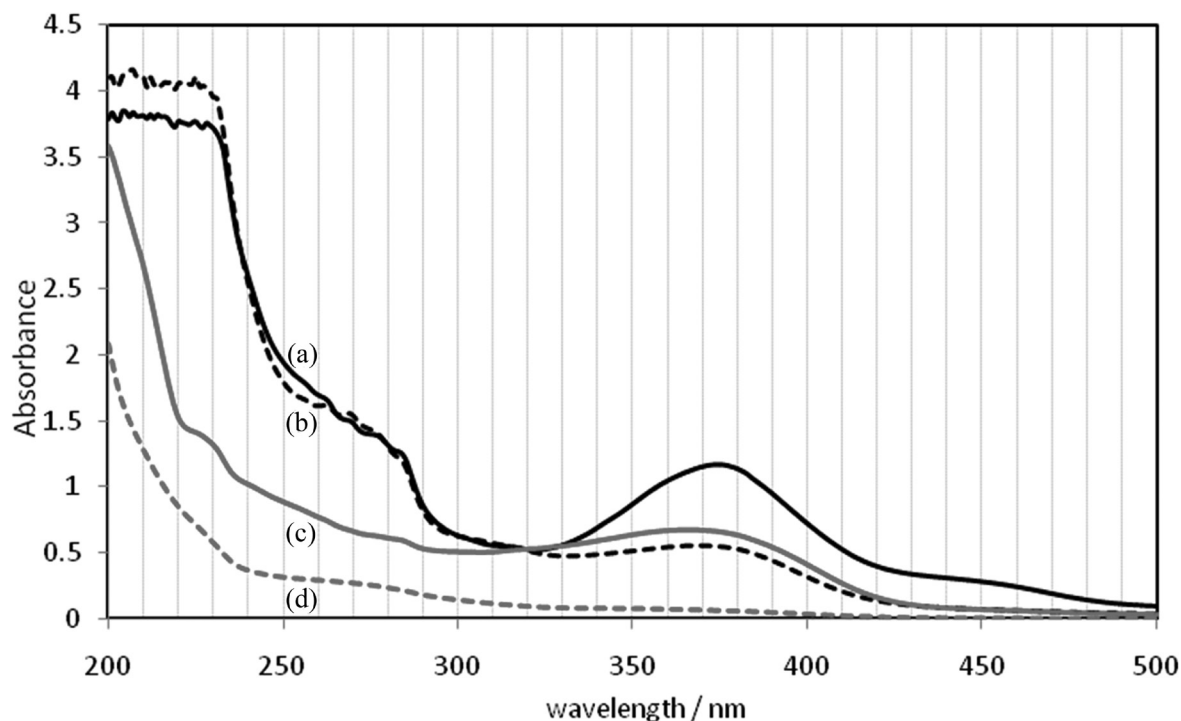
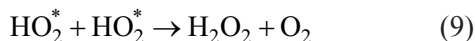
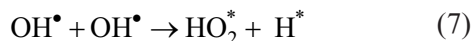
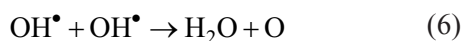
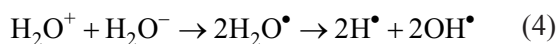
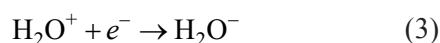
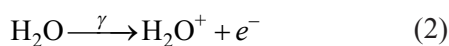
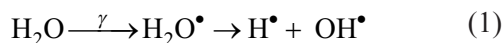


Figure 1. UV spectra of 1:9 dilution a) no irradiation and no catalyst, b) no irradiation and catalyst, c) no catalyst and irradiated at 15 kGy, d) with catalyst and irradiated at 15 kGy.

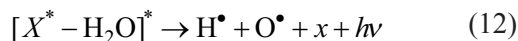
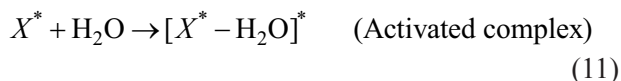
tivities from these transitions are relatively low and show an absorbance region of the spectrum in 270–300 nm. Then, this kind of compounds is proposed to be adsorbed by the catalyst.

The residual organic concentration of the irradiated samples is showed in Figures 1(c) and 1(d), where, in both regions, lower absorbance was observed. However, again, absorbance in region 373 nm was lower than in 254 nm. From this, several considerations must be taken into account.

The radiolysis of water appears as follow [11,17]:



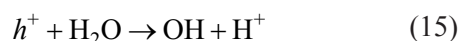
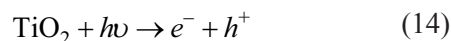
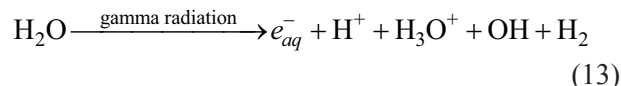
In the presence of the catalyst, the radiocatalysis can be represented as follow: [11,17]



Irradiation of heterogeneous systems often leads to an effective redistribution of absorbed radiation energy between contacting phases. The energy of ionizing radiation adsorbed in one phase can be delivered to the interface and can induce physical and chemical processes in the other phase. The energetic efficiency of the adsorbed molecule radiolysis should be attributed to the energy absorbed by the molecule directly or in-

directly delivered by the catalyst. This redistribution from primary energy absorption (i.e., gamma radiation) and the final radiation-induced chemical reaction event is separated in space and time. The energy migration between these points is conducted mostly by the highly energetic secondary electrons, hot carriers, and thermalized particles or excitations [18].

Ionizing radiation can influence systems in different ways. At first, the effect of radiation over catalysts that result in variations in structural and electronic imperfections [18] and the effect of radiation in solution where electronically excited as a sequence of interaction between ionizing radiation with water and dissolved oxygen, thus forming ionized molecules. On the other hand, the degradation by radiocatalysis is, conceptually, a combination of radiolysis and heterogeneous photocatalysis, two processes that generate $\bullet\text{OH}$ radicals [6,7].



It is proposed that radiocatalysis is an extension of photocatalytic processes that occur with ionizing radiation, Equation (13). In these processes, the energy is absorbed by the catalyst (semiconductor) as titanium dioxide, Equation (14), causing the formation of a pair of electron-holes (e^-/h^+) and the posterior formation of radicals as the $\bullet\text{OH}$, Equations (15) and (16) [10,13].

In the case of TiO_2 , it is commonly accepted that holes formed by ionizing radiation are transformed into hydroxyl radicals ($\bullet\text{OH}$) and, in the presence of dissolved molecular oxygen, e_{aq}^- is converted into the superoxide anion ($\bullet\text{O}^-$). It is generally assumed that $\bullet\text{OH}$ radicals are the major species responsible for the mineralization of organic pollutants [20].

Photocatalysis allows the oxidation of almost all organic and inorganic compounds at room temperature and pressure up to negligible concentration levels. Therefore, photocatalysis represents a promising alternate technology for the degradation of environmental pollutants present in water or air and for the inactivation of microorganisms in water. Since very few species are refractory to photocatalytic oxidation,

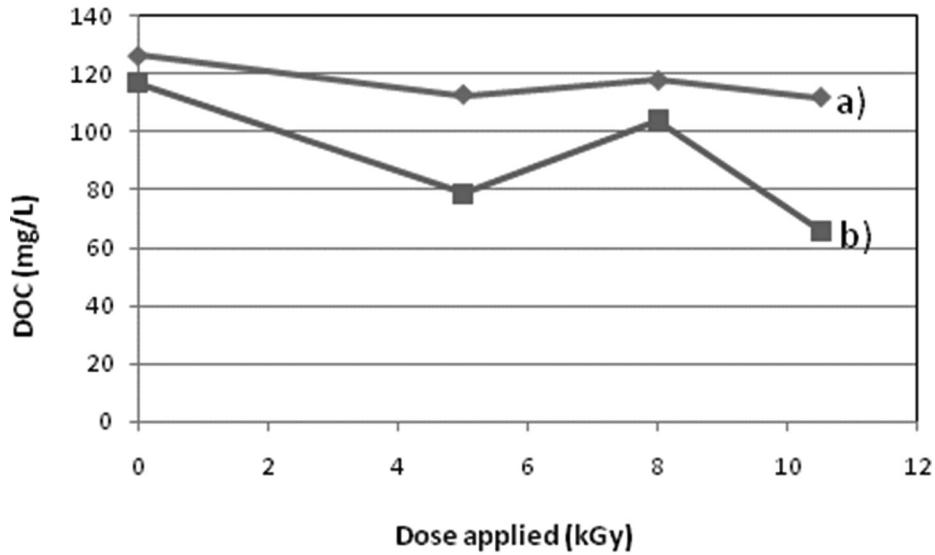


Figure 2. UV₂₅₄ as DOC for sample dilution 1:9 in function of dose applied, a) no catalyst, b) with catalyst.

this technology is considered greatly unselective. This consideration could be taken also for radiocatalysis.

From this consideration and, possibility, from the consideration of different adsorptions of organic compounds and the formation of byproducts of degradation reactions, only an analysis was made as mean UV absorption at 254 nm (UV₂₅₄). Because many organic

compounds in water and wastewater do not absorb significantly in UV wavelengths, there is a correlation between UV absorption at 254 nm and dissolved organic carbon (DOC).

When a high gamma irradiation dose is applied, TiO₂ particles have no significant effect on organic degradation. It is probably induced by water decompo-

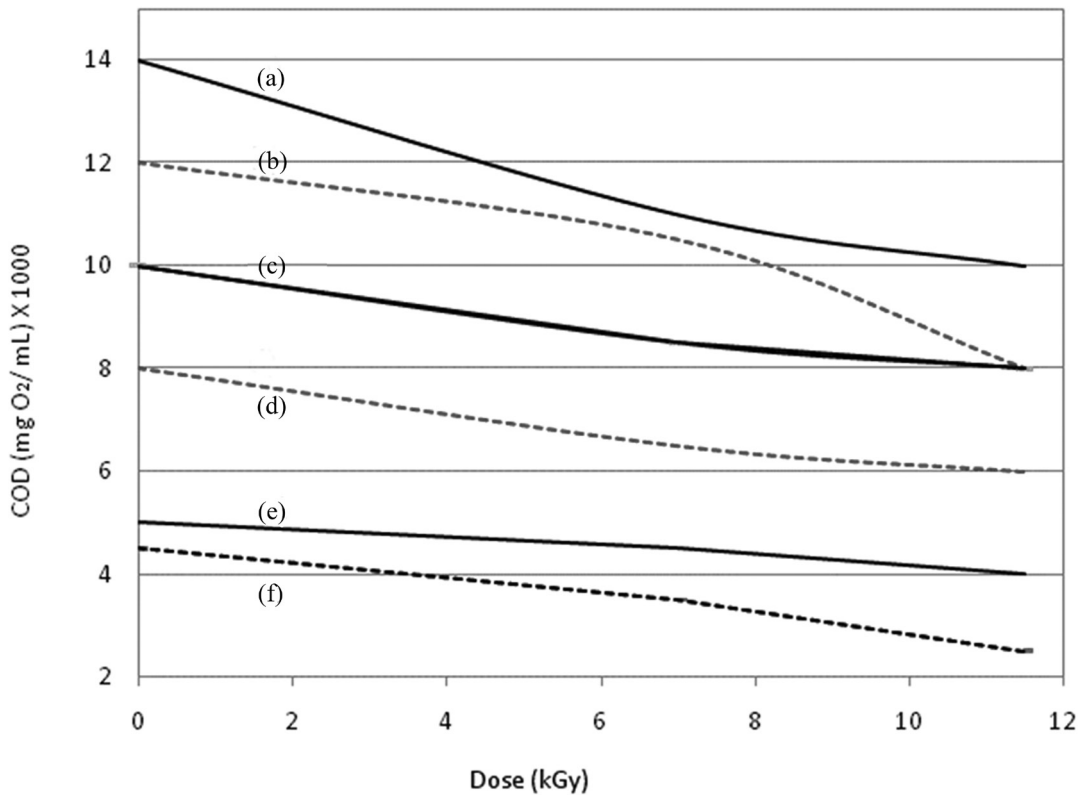


Figure 3. COD remained after gamma irradiation of penetrant liquid waste residual dilutions; (a) 3:7, no catalyst, (b) 3:7, catalyst, (c) 2:8, no catalyst, (d) 2:8, catalyst, (e) 1:9, no catalyst and (f) 1:9, catalyst.

sition products [7,10]. In the present study, the sample solutions were saturated with air and were not stirred. A decrease in the oxygen concentration may lead to some variations in the yields [21].

Doses applied in this study were lower than in previous studies so the effect of the addition of TiO₂ could be monitored. Figure 2 shows that all samples with TiO₂ had lower residual organic compounds than the only-irradiated samples [22].

Another function of TiO₂ is the catalytic effect due to the large surface area. This can trap hydroxyl radicals with a lifetime much longer than that of the bulk solution.

The result of the effects of the doses applied is shown in Figure 3. When the doses were increased, although with great variations, in all cases the absorbance decreased, which suggests a degradation of the compounds. A general tendency is that when the dose is increased, degradation increases for radiolysis, radiocatalysis, or both processes. These results are compatible with enhanced degradation observed in radiocatalysis compared with the absence of a catalyst.

The measures of chemical oxygen demand (COD) are often applied to monitor the decrease of organic content. This value represents the total concentration of substances that can be chemically oxidized into inorganic products.

In order, Figure 3 presents the results of COD of the degradation by radiocatalysis. The effect of the dose of degradation by radiocatalysis was evident in the case of more diluted samples with a high degradation with respect to other samples.

In radiolysis, the direct degradation of the compound occurs with increases in the concentration. Figure 3 shows major degradation of the diluted solution, which suggests that degradation for •OH radicals is more efficient than the direct degradation of the compound.

The radiocatalysis is also higher than that obtained by radiolysis gamma (see Figure 3). The degradation achieved was on the order of 30% to 50%. This efficiency can be increased with a major dose of gamma radiation and the amount of catalyst or a combination with other advanced oxidation processes to dispose of the penetrant liquid waste.

CONCLUSIONS

Based on early studies, the gamma irradiation in the presence of a catalyst as TiO₂ improves the generation of radicals in molecular products enhances the degradation of organic compounds. The radiocatalysis

improves the degradation of the penetrant liquid waste at efficiencies of 20% to 44%. The results show degradation mainly for the interaction with •OH radicals generated by radiolysis and radiocatalysis. Major degradation was observed with the use of radiocatalysis gamma irradiation. Efforts involving this technique can be done in order to improve waste degradation.

REFERENCES

1. ASTM, (American Standard for Testing Materials) ASTM E165 / E165M - 12 *Standard practice for liquid penetrant examination for general industry*, ASTM International, West Conshohocken, PA, 2009. DOI: 10.1520/E0165_E0165M-12
2. Paquin L.A., Gilliland K., "Indiana bridge inspection manual", in *Indiana Department Of Transportation* (INDOT), 2010. http://www.in.gov/dot/div/contracts/standards/bridge/inspector_manual/BridgeInspection-ManualFinal11.pdf
3. Cevinini, M., "New water base liquid penetrant. What changes", in *NDT ITALIANA srl Via del Lavoro, 28 - 20863 Concorezzo (MB) IT-ALY*, 2012. <http://www.ndt.it/uk/waterbase.pdf> Accessed 10 May 2013.
4. Alinsafi, A., Evenou, F., Abdulkarim, E.M., Pons, M.N., Zahraa, O., Benhammou, A., Yaacoubi, A., Nejmeddine, A., "Treatment of textile industry wastewater by supported Photocatalysis", *Dyes Pigments*, Vol. 74, No. 2, 2007, pp. 439-445.
5. Meas, Y., Ramírez, J.A., Villalon, M.A., Chapman, T.W., "Industrial wastewaters treated by electrocoagulation", *Electrochim. Acta*, Vol. 55, No. 27, 2010, pp. 8165-8171.
6. Jay-Gerin, J.P., Ferradini, C., "A new estimate of the •OH radical yield at early times in the radiolysis of liquid water", *Chem. Phys. Lett.*, Vol. 317, No. 3-5, 2000, pp. 388-391.
7. Chitose, N., Ueta, S., Seino, S., Yamamoto, T.A., "Radiolysis of aqueous phenol solutions with nanoparticles. I. Phenol degradation and TOC removal in solutions containing TiO₂ induced by UV, gamma-ray and electron beams", *Chemosphere* Vol. 50, No. 8, 2003, pp. 1007-1013.
8. Essehli, R., Crumiere, F., Blain, G., Vandenborre, J., Pottier, F., Grambow, M., Fattahi, M., Mosrafavi, M., "H₂ production by γ and He ions water radiolysis, effect of the presence TiO₂ nanoparticles", *Int. J. Hydrogen Energy*, Vol. 36, No. 22, 2011, pp. 14342-14348.
9. Palfi, S., Sarkany, A., Tetenyi, P., "The effect of γ -radiation energy transfer in the radiocatalytic decomposition of 2-propanol", *Radiat. Phys. Chem* (1977), Vol 19 No. 6, 1982, pp. 485-489.
10. González-Juárez, J., Jiménez-Becerril, J., "Gamma radiation-induced catalytic degradation of 4-chlorophenol using SiO₂, TiO₂, and Al₂O₃", *Radiat. Phys. Chem.*, Vol. 75, No. 7, 2006, pp. 768-772.
11. Kralchevska, R., Milanova, M., Tsvetkov, M., Dimitrov, D., Todorovsky, D., "Influence of gamma-irradiation on the photocatalytic activity of Degussa P25 TiO₂", *J. Mater. Sci.*, Vol. 47, No. 12, 2012, pp. 4936-4945.
12. Candal, R.J., Bilmes, S.A., Blesa, M.A., "Capítulo 4. Semiconductores con actividad fotocatalítica", in: M.A. Blesa (Ed.). *Eliminación de contaminantes por fotocatalisis heterogénea*, Comisión Nacional de Energía Atómica, Argentina, 2001, pp. 77-101.
13. Yamaguchi, H., "A spur diffusion model applied to estimate yields of species in water irradiated by monoenergetic photons of 50eV-2MeV", *Inter. J. Radiat. Applications Instrumentation. Part C. Radiat. Phys. Chem.*, Vol. 34, No. 5, 1989, pp. 801-807.
14. Cano-García, G., Martínez-Hernández, A., Jiménez-Becerril, J., "Use of TiO₂ as catalyst in degradation induced with gamma radiation of methylene blue", *J. Chem. Soc. Pakistan*, Vol. 34, No. 3, 2012, pp. 533-535.
15. USEPA Method 415.3 "Determination of Total Organic Carbon and Specific UV Absorbance at 254 nm in Source Water and Drinking Water". Revision 1.1, February, 2005
16. ISO 6060:1989(E), "Water quality—Determination of the chemical

- oxygen demand". Second edition. International Organization for Standardization
17. Cecal, A., Goanta, M., Palamaru, M., Stoicescu, T., Popa, K., Paraschivescu, A., Anita, V., "Use of some oxides in radiolytical decomposition of water", *Radiat. Phys. Chem.* Vol. 62, No. 4, 2001, pp. 333–336.
 18. Petrik, N.G., Alexandrov, A.B, Vall, A.I., "Interfacial energy transfer during gamma radiolysis of water on the surface of ZrO_2 and some other oxides", *J. Phys. Chem. B.*, Vol. 105, No. 25, 2001, pp. 5935–5944.
 19. Abd El All, S., Ali El-Shobaky, G., "Structural and electrical properties of γ -irradiated TiO_2/Al_2O_3 composite prepared by sol-gel method", *J. Alloys Compounds*, Vol. 479, No. 1–2, 2009, pp. 91–96.
 20. Schwarz, P.F., Turro, N.J., Bossmann, S.H., Braun, A.M., Abdel Wahab, A.M.A, Durr H., "A new method to determinate the generation of hydroxyl radicals in illuminated TiO_2 suspensions", *J. Phys. Chem. B.*, Vol. 101, No. 36, 1997, pp. 7127–7134.
 21. Getoff, N., "Radiation-induced degradation of water pollutants—state of the art", *Radiat. Phys. Chem.*, Vol. 47, No. 4, 1996, pp. 581–593.
 22. Coekelbergs, R., Crucq, A., Frennet, A., "Radiation Catalysis", In: D.D. Eley, P.W. Selwood, Paul B. Weisz, A.A. Balandin, J.H. De Boer, P.J. Debye, P.H. Emmett, J. Horiuti, W. Jost, G. Natta, E.K. Rideal and H.S. Taylor, Editor(s), *Advances in Catalysis*, Academic Press, 1962, Vol. 13, pp. 55–136.

Hydrothermal Carbonization of Organic Material with Low Dry Matter Content: The Example of Waste Whey

M. ESCALA¹, A. GRABER¹, R. JUNGE¹, CH. KOLLER¹, V. GUINÉ² and R. KREBS^{1,*}

¹*Institute of Natural Resource Sciences, ZHAW, Campus Grüental, CH-8820, Wädenswil, Switzerland*

²*Laboratory of Soils and Substrates, HEPIA, 150, route de Pressinge, 1254 Jussy, Geneva, Switzerland*

ABSTRACT: Hydrothermal carbonization at 205°C was evaluated to process waste whey containing 5.9% of dry matter to a coal-like material and process water. Carbonization increased dramatically the heating value, with 15.0 MJ/kg for whey and 25.2 MJ/kg for coal, alongside the carbon fraction, from 38.0% (whey) to 60.4% (coal). Carbonization brought C/H and C/O molar ratios to typical values for brown coal. HTC process water showed a low N/P ratio, and could thus be interesting as phosphorus fertilizer. However, elevated concentrations of phenols and cyanides suggest that further treatment might be necessary.

INTRODUCTION

RECENTLY, new strategies are being discussed in order to implement environmentally clean technologies, process residuals, and decelerate climate change [1,2]. A key feature in this context is the correct management of the biomass both in its natural state and as residuals.

Titirici et al. recently presented the idea of using the laboratory analogue for natural coalification to process wet biomass to a fuel [3]. This process known as hydrothermal carbonization or HTC consists of heating up biomass in presence of water to temperatures around 180–210°C in a closed vessel and thus allowing for saturated pressure to build up. The hydrothermal carbonization includes several reaction mechanisms and mainly hydrolysis, dehydration, decarboxylation, polymerization, and aromatization. Although, the detailed reaction characteristics are only known for a few compounds such as cellulose [4]. Reaction products of HTC consist mainly of a solid and liquid phase (HTC-coal and process water, respectively) with only a small amount of gas (mainly CO₂). The HTC-coal typically shows characteristics of brown coal and may be used as an energy carrier [4], thus providing an easily stored fuel with a CO₂-neutral balance and in some cases also as a soil conditioner [5]. A third application of the HTC-coal is the synthesis of carbon-based materials

with specific properties [6]. Therefore, HTC can also offer a solution for the treatment of organic industrial or agricultural by-products that are produced in large quantities or generated in isolated areas.

Whey is a by-product of the cheese industry, obtained from milk after removing fat and casein. The worldwide production of whey from cow milk is estimated to be over 100 million tons per year and about 50% of this in Europe [7]. Whey is a nutritious liquid, containing whey proteins, lactose, vitamins and minerals as well as some enzymes, hormones and growth factors. In Europe, around 25% of the whey is used as supplement in food products, which usually requires intermediate processes such as demineralization, fractionation, delactozation or isolation [7]. Another fraction of whey is used as pig feed. However, the amount of whey that can be used for nutrition is limited due to the side effects that an excess of whey can cause, for instance, pH disorders and intestinal toxemia. Therefore, whey disposal is often considered a problem [8]. Furthermore, it is occasionally transported out of the dairy plant for a per volume charge, which results in high disposal costs.

This study aims at evaluating hydrothermal carbonization to process whey to a fuel and process water potentially useable as a fertilizer. To our best knowledge this is the first report on the carbonization of whey; thus the focus is on determining the composition and properties of the obtained products, namely HTC-coal and process water, as well as investigating the energy balance and the effect of different carbonization times.

*Author to whom correspondence should be addressed.
E-mail: rolf.krebs@zhaw.ch

MATERIAL AND METHODS

Whey

Whey (3 L, 5.9% dry weight, Figure 1) was collected from a cheese dairy (Unterägeri, Switzerland) and kept at 4°C in a glass bottle wrapped in aluminum foil to exclude light. The carbonization experiments and the subsequent analyses were performed within 10 days after collection.

Reactor

A 250 mL stainless steel autoclave (ROTH *Hochdruck-Laborautoklav* Modell II) with an in-built electrical mantle heating system and magnetic stirring was used for the carbonization. The reactor was operated in a room kept at 20°C.

Hydrothermal Carbonization Reactions

A glass cylindrical flask was filled with 150 mL of whey and a magnetic stirrer and introduced in the reactor. 25 mL of distilled water were added between the glass flask and the reactor wall to improve heat conduction. A total of 7 carbonization reactions were performed in which the autoclave was heated to the target temperature of 230°C. As a convention, the carbonization time measurement started when the tempera-



Figure 1. Whey from a Swiss cheese dairy. Input material to the hydrothermal carbonization process with 5.9 % dry weight.

ture reached 205°C and stopped when the reactor was switched off. The carbonization time for the 7 experiments was 0.08 h, 0.6 h, 2.2 h (three repetitions), 3.8 h, and 5.8 h, respectively. The corresponding pressure at 205°C was 2.1 MPa. The maximum temperature and pressure reached in an experiment were 218°C with a corresponding pressure of 2.6 MPa. After each carbonization the autoclave was switched off and allowed to cool overnight, which resulted in a final residual pressure of 0.25 to 0.48 MPa. The HTC-coal and the process water were separated by centrifugation (10 min, 4400 rpm) followed by decantation. The HTC-coal was dried in an oven at 60°C, grinded and homogenized in a swing mill (3 min at 17 Hz), and subjected to further analyses. Water samples were wrapped in aluminum foil, stored in a refrigerator, and analyzed within 24 hours after each experiment.

HTC-Coal and Process Water Analysis

HTC-Coal

Elemental analysis (C–H–N–O, precision 0.3%) and heating value of HTC-coal (precision 120 kJ/kg) were conducted for the samples carbonized during 0.5, 3.8, and 5.8h to investigate influence of carbonization time on composition of biomass. For pH measurement, 1.25 g of HTC-coal were diluted with 20 ml of demineralized water and mixed for 24 hrs. The pH was then determined by Orion® 920 A pH-meter. Particle size distribution was achieved by hand sieving dry HTC-coal in metals sifters (sizes: 50 µm, 500 µm, 2 mm).

Process Water

Electric conductivity (EC) and pH-value were determined with multi-parameter digital meter (HQ40d, HACH LANGE) in a homogenized sample of the process water without prior filtering and/or sedimentation. For further determinations the particles in the process water were allowed to sediment for approx. 10 min before pipetting the sample from the upper layer of the supernatant.

Total phosphorus (TP), total nitrogen (TN), ammonium nitrogen (NH₄-N), potassium (K), total phenol, and cyanide content were determined photometrically (DR 3800, HACH LANGE). NH₄-N and K were analyzed after sterile filtration (0.45 µm glass fiber pre-filter) using LCK 304 and LCK 328, respectively. TP and TN (assays LCK 349 and LCK 138, respectively) were measured in a non-filtered solution. Samples were sub-

jected to thermal hydrolysis in thermostat (HT 200S) for 1 hr at 100°C. Phenols (LCK 345) were also analyzed in non-filtered samples using only glassware and under exclusion of light. Prior to determination of total cyanides (LCK 319), pH was adjusted to 7–10 with a 5% sodium hydroxide solution.

The appropriate dilution of the original sample that would comply with the measurement range of the method was determined by diluting process water with ultrapure water (Water HPLC, PH Stehelin), resulting in dilutions from 1:10 to 1:1000 which were then analyzed. Regarding subsequent analyses the dilutions which gave readings in the lower third of the measurement range of the analysis method were used. These were 1:10 for cyanide, 1:100 for potassium, 1:500 for total phenols, total nitrogen and ammonium nitrogen, and 1:1000 for total phosphorus. Extinction value of the sample background color was zero for all dilutions.

Carbon Balance

Distribution of carbon in the HTC products was compiled from the carbon fraction and TOC analyzed in the HTC-coal and process water respectively. The gas phase was not analyzed, but the carbon content was estimated using the ideal gas law. As an example, for the 0.6 h experiment, the reactor was opened at 79°C and with 0.34 MPa of residual pressure in a headspace volume of approximately 100 mL. At 79°C the water vapor pressure is 0.05 MPa. Assuming that the remaining 0.29 MPa are entirely carbon dioxide, the number of carbon dioxide moles present in the gas phase is: $n = (P \times V)/(R \times T)$; where n is the number of moles, P is the pressure (0.29×10^5 Pa), V is the volume in the reactor headspace (100×10^{-6} m³), R is the ideal gas constant (8.31 J mol⁻¹ K⁻¹), and T is the temperature (352 K). This results in 0.01 moles of carbon dioxide with 12 g mol⁻¹ of C = 0.1 g C in the gas phase. In reality the amount of C in the gas might vary since other species other than carbon dioxide might be present (CH₄, CO, H₂, and traces of CmHn). Although, studies have confirmed that these are in minor concentrations in comparison to carbon dioxide (Funke and Ziegler, 2010, and references therein).

RESULTS AND DISCUSSION

HTC-Coal

The products obtained from carbonization of whey were a black coal-like material (Figure 2) and a black

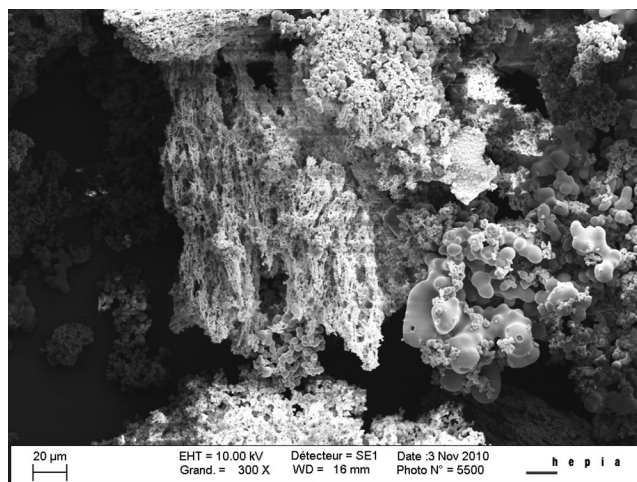


Figure 2. Structure of HTC-coal. Representative HTC-coal obtained by the carbonization of whey in scanning electron microscope (Zeiss® LEO 1455VP) 300-times magnified.

fluid phase or process water, as well as a minimum amount of gas responsible for the residual pressure in the reactor. The pH of HTC-coal was 4.9 after carbonization.

The solid yield slightly increased with carbonization time from 45.8% (0.08 h) to 53.9% (6h), calculated as the ratio between HTC-coal dry weight and whey dry weight. This corresponds to an increase from 2.7% to 3.2% of HTC-coal (d.w.) obtained from fresh whey (Figure 1), with as much increase in the first 2 hours of carbonization as with additional 3 hours. A reduction of the solid content after carbonization is expected, as an important and early reaction during the whole process of carbonization is dehydration, during which alcohol groups and hydrogen atoms are detached from the molecules thus resulting in a loss of mass.

Particle size distributions of HTC-coal (Figure 3) carbonized for 2.2h and 3.8h, respectively, were similar with 89% of particles smaller than 50µm and 11% smaller than 500 µm.

The carbon fraction found in coal increased strongly in the first minutes of carbonization, from 38.0% (whey) to 60.4% (0.08 h) and again increased only slightly with further carbonization time, reaching 65.5% after 6 h (Table 1). Oxygen content decreased from 46.8% in the whey to 21.4% after 6h of carbonization (Table 1).

Similarly, carbonization of whey changed dramatically the heating value of the substance from 15.0 MJ/kg for whey to 25.2 MJ/kg after only 0.08 h of carbonization. Only a mild effect was identified on heating value as carbonization time increased with a maximum of 30.1 MJ/kg observed after 4 h (Figure 4).



Figure 3. HTC char. Separated and dried output material of carbonized whey after 3.8 h carbonization time.

Degree of carbonization has been previously shown to increase with increasing severity of the reaction (i.e., increasing temperature and/or time). Although, the interaction between these two parameters is still not well understood [4]. In the present study, the effect of increasing carbonization time was associated with a decrease in molar ratios between hydrogen and carbon and between oxygen and carbon in the coal: initial ratios were 1.99 and 0.92, respectively, while final ratios were in the range 1.02–1.16 for H/C and 0.24–0.31 for O/C (Figure 5). These values correspond to natural brown coal for which H/C between 0.8–0.9 and O/C between 0.2–0.3 were reported [21]. Furthermore, geothermal maturity of coal in nature is evidenced by a progressive decrease of these two ratios [22] which can be to a great extent explained by dehydration as part of the carbonization process [4]. It is worth noting that only 0.6 h carbonization time was enough to bring these molar ratios into the area of typical values for brown coal while extending carbonization to 3.8 h and 5.8 h provided little additional change.

These results suggest that whey can be readily carbonized. In fact, approximately 72% of the solid content of whey is composed by carbohydrates (lactose)

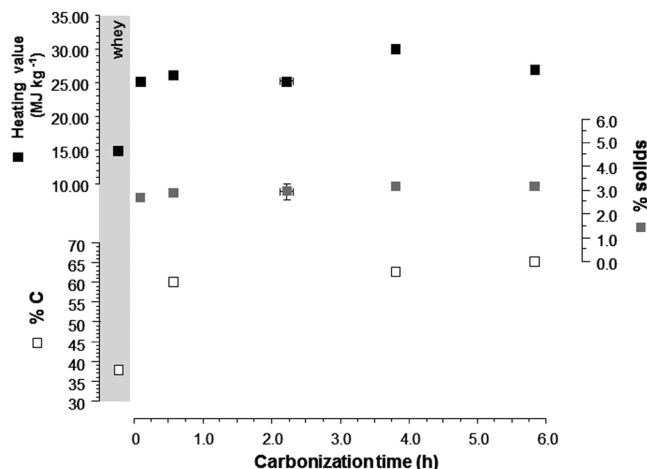


Figure 4. Heating value, % solids and %C in solids for dried whey and the carbonized whey samples. The experiment with 2.2 h carbonization time includes three replicate samples, error bars show 15.

which are highly soluble and amenable for hydrolysis [7,3]. In this regard the relatively high temperature (ca. 205°C) at which the hydrothermal carbonization was conducted in this study is probably the dominating factor in the reaction with time being only a minor factor.

Process Water

The pH of the process water was more acidic than that of original whey (pH = 4.59) and showed a slight trend of weaker acidification with longer carbonization time (i.e., pH = 3.49 for 0.08 h carbonization to pH = 3.97 for 5.8 h carbonization). The acidic nature of whey is probably enhancing the HTC reactions while acidification during the process is in agreement with previous carbonization experiments [4].

Concentration of all components in the process water resulting from hydrothermal carbonization was very high (Table 2). Variation of single parameters among the different batches was up to 22%, except for nitrite. Prolonged carbonization time resulted in small changes in the concentrations of substances (Figure 6). Total phosphorus and nitrogen and ammonium remained stable, so that the N/P atomic ratio remained

Table 1. Elemental Composition of the Whey and HTC-Coal Carbonized at 205°C in Dependence of Carbonization Time.

Sample	Carbonization Time (h)	C (% mass)	H (% mass)	O (% mass)	N (% mass)
Whey	0	38.0	6.3	46.8	2.2
HTC coal fast	0.6	60.4	5.8	24.9	3.1
HTC coal medium	3.8	63.0	5.4	23.2	3.2
HTC coal slow	5.8	65.5	6.3	21.4	3.2

Table 2. Composition of the Process Water Resulting from Hydrothermal Carbonization of Whey During 2.2 h Reaction Time.

Parameter/Sample	Unit	2h17'	2h11'	2h06'	Mean	st.dev.	CV %
EC	μS/cm	7140	7209	7043	7131	83	1
pH	–	3.75	3.77	3.78	3.77	0.02	0
TOC	mg/l	6050	8850	6367	7089	1533	22
DOC	mg/l	5925	8017	5867	6603	1225	19
Cyanide	mg/l	0.42	0.45	0.47	0.45	0.02	5
Phenols	mg/l	318	415	320	351	55	16
Total-P	mg/l	259	243	207	237	27	11
Total-N	mg/l	443	486	470	466	22	5
Ammonium	mg/l	82	100	86	89	9	10
Nitrite	mg/l	0.69	0.28	0.34	0.44	0.23	52
Potassium	mg/l	1320	1217	1170	1236	77	6

stable at 4.6 and data range from 3.8 to 5.2. Concentration of phenols and potassium increased from 0.08 h to 0.6 h carbonization time. Subsequently phenol concentration dropped continuously (Figure 7) whereas potassium values remained stable.

The N/P atomic ratio of whey is approximately 6.8 and calculated from [23]. It may be postulated that phosphorus and nitrogen are preferentially sequestered into the process water during the early stage of carbonization. Elimination of phenols suggests decomposition due to harsh process conditions or a constant adsorption on the HTC-coal.

The resulting process water from whey carbonization is to some extent comparable to process water from biomass mechanization plants [24,25] and to wash water from wood gasification process [26] (Table 3). The largest differences were in N/P atomic ratio whereas HTC process water has a low N/P ratio and could thus be an interesting as a source of phosphorus fertilizer. Other types of wastewater, especially wash water from

gasifiers, have extremely unsuitable ratios. Depending on the parameter observed it was up to several thousand times higher than values allowed for drinking water [27], and up to several hundred times higher than discharge requirements for communal wastewater treatments plants [28].

Whereas, concentrations of macronutrients suggest that this water could be used as a fertilizer. Elevated values of phenols and cyanides suggest that this is potentially toxic water. Therefore, these two substances should be removed prior to any recycling application.

Carbon Balance

Distribution of the carbon in the HTC products may be observed in Figure 8. For the three experiments (0.6 h, 4 h and 6 h) the amount of C in the HTC-coal is between 65% and 75% while the process water contains 21% to 31% of the carbon and only a residual part (2% to 4%) is calculated to be in the gas phase. It must be

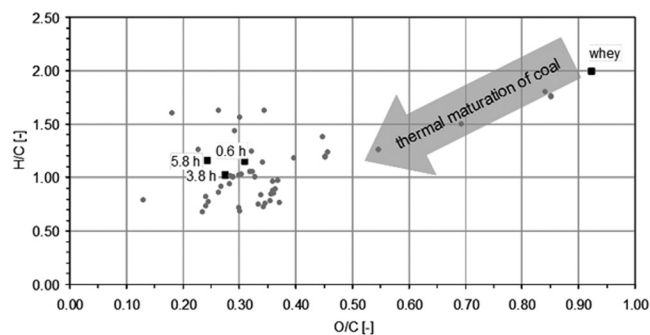


Figure 5. Chemical composition of whey and HTC-coal. Van Krevelen diagram with the chemical composition of whey (black squares) before and after carbonization (1). Additional experimental data from carbonized samples comes from [10] and from A. Funke (TU Berlin, Germany, who provided data for the following references: [11], [12], [13], [14], [15], [16], [17], [18], [19], [20], from which only samples carbonized at temperatures between 180 and 230 °C are represented).

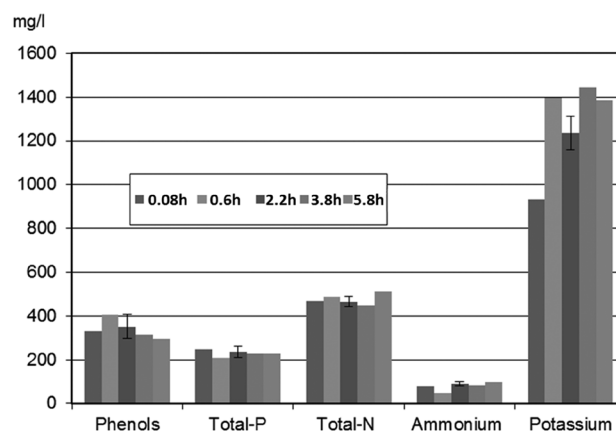


Figure 6. Process water composition. Changes in composition of process water in dependence of carbonization time.

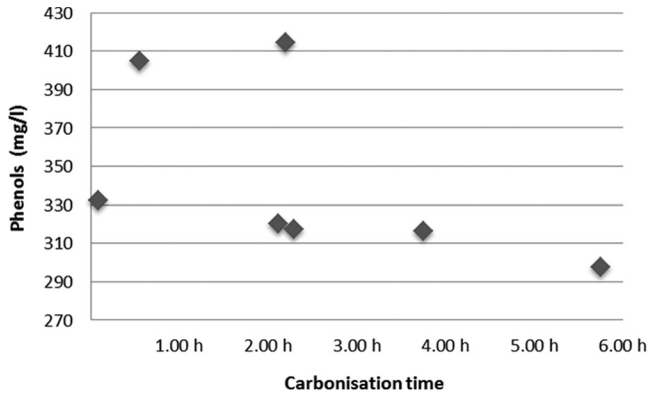


Figure 7. Phenols in process water. Concentration of phenols in the process water in dependence of carbonization time.

noted that a small part of the C accounted for in the HTC-coal could actually belong to process water as after centrifugation there is still part of the water absorbed in the coal and its C content is eventually found in the dried coal.

From the point of view of the carbon management the small carbon fraction in the gas phase is a desirable result of the HTC while the relatively high amount of carbon in the process water poses a new challenge. A solution of carbon is not amenable for energy recover.

Energy Balance

A key point in the revaluation of waste products is the energetic efficiency of the process. Energy invested in carbonization should be less than energy that can be harnessed from biomass or that may be saved by modifying traditional treatment of this biomass. Otherwise,

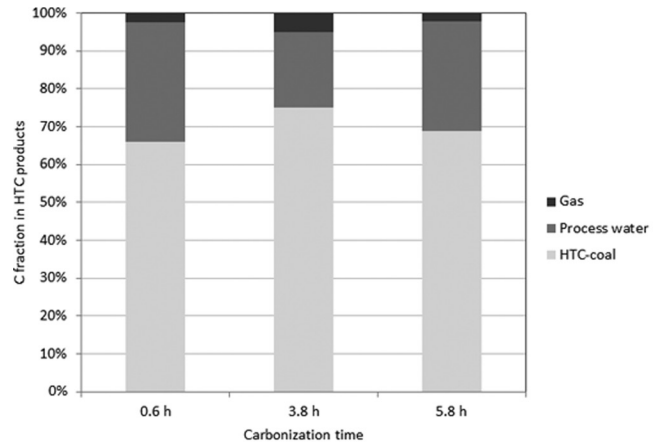


Figure 8. Carbon balance. Distribution of carbon in the hydrothermal carbonization products.

the process does not make sense from an environmental point of view unless other problems associated to the biomass (e.g. pathogen activity) are solved by carbonization. Here in this study the energetic efficiency of the HTC process and subsequent combustion of HTC-coal was calculated for 1 kg of whey using experimental data as well as reference data from literature.

Step 1: Heating 1 kg (m) of whey from 20°C to 205°C ($\Delta T = 185^\circ\text{C}$). Heat capacity of whey (C_{whey}) is $4.05 \text{ J g}^{-1} \text{ }^\circ\text{C}^{-1}$ [29]. Enthalpy of this step was $\Delta H_{\text{step 1}} = m \times C_{\text{whey}} \times \Delta T = 0.750 \text{ MJ kg}^{-1}$.

Step 2: Centrifugation of the coal/process water slurry and decantation of water: this energy is neglected [10]. After centrifugation a solid phase with 14% dry weight was obtained (experimental data). The output was therefore 227 g of wet HTC-coal.

Step 3: Drying the 227 g of wet HTC-coal to remove 195 g of water (m) and obtain HTC-coal with 100%

Table 2. Composition of the Process Water Resulting from Hydrothermal Carbonization of Whey Compared with Different Types of Nutrient-rich Wastewaters.

	Unit	HTC-whey-Process Water (2 h)	Biogas Process Water ⁽¹⁾	Liquid Cattle Manure ⁽³⁾	Washwater from a Wood Gasifier ⁽⁴⁾
Electric conductivity	mS/cm	7.13	4–12 ⁽²⁾	30.5	3.00
pH	–	3.77	8.2	7.63	7.21
Total Phosphorus	mg/l	237	794	78	0.3
Total Nitrogen	mg/l	466	2982	>1810	770
Ammonium-Nitrogen	mg/l	89	1595	1650	374
Potassium	mg/l	1,236	3,724	13,000	16
Total Phenols	mg/l	351	–	–	182
Total-Cyanide	mgCN/l	0.45	–	–	0.28
N/P atomic ratio	–	4.74	3.8	>23	2560

⁽¹⁾Mechanically pretreated process water from biomass methanisation plant Kompogas® [29].

⁽²⁾Graber and Junge-Berberovic [30] and unpublished data.

⁽³⁾Liquid cattle manure from a dairy farm in Switzerland (2002, unpublished data).

⁽⁴⁾Wash water from wood gasification process [31], standardised by diluting to 3000 $\mu\text{S/cm}$.

dry weight. Assuming that the heat of the biomass in the reactor can be used to heat up the centrifuged HTC-coal to 100°C, energy is only necessary to vaporize water ($\Delta H_{\text{vaporization}}$ at 373 K = 2.26 MJ kg⁻¹). Thus the enthalpy of this step was $\Delta H_{\text{step 3}} = m \times \Delta H_{\text{vaporization}} = 0.442 \text{ MJ kg}^{-1}$.

Step 4: Heat obtained from burning the 32 g (m) of dry HTC-coal obtained. Assuming a lower heating value of $H_v = 26.4 \text{ MJ kg}^{-1}$ (experimental data) the enthalpy of this step was $\Delta H_{\text{step 4}} = H_v \cdot m = 0.838 \text{ MJ kg}^{-1}$.

The final balance of the process was $\Delta H_{\text{process}} = 0.750 + 0.442 - 0.838 = 0.353 \text{ MJ kg}^{-1}$ that needed to be invested for whey (dry weight 5.9%) to be carbonized and burned. The energy balance shows that carbonizing pure whey to use it as energy vector is not reasonable. The main reason is the large amount of water that needs to be heated (and evaporated) at the beginning and end of the process. However, if the heat of the reactor content could be reused with an efficiency of 55%, the balance would be neutral, given that an additional 0.4 MJ kg⁻¹ would enter the calculation as a gain. The efficiency with which heat can be recovered largely depends on the infrastructure and technology used; in this study the heat recovery was not further investigated with the laboratory-scale reactor. On the other hand, whey is highly amenable for carbonization and undergoes a rapid transformation at 205°C. Therefore, it would be interesting to carbonize it together with drier biomass, such as agricultural “waste” biomass or domestic organic waste, because it would add the water required for the hydrothermal process as well as readily carbonizable carbohydrates.

CONCLUSIONS

Hydrothermal carbonization of organic waste is an option for its revaluation as an energy vector in the form of HTC-coal with a higher energy density than the original product. As seen in this study on the example of whey, educts with a high content of water can be carbonized under relatively mild conditions (205°C) and extremely fast reaction times less than 0.5 hrs. The energy balance is only attractive if at least 55% of the heat in the reactor can be recycled. Otherwise, the high water content requires a large quantity of energy to be evaporated. Therefore, further research should also focus on identifying suitable mixtures of whey with drier biomass for its carbonization. Substitution of conventional coal with HTC-coal should also receive special attention as this would imply a net reduction of CO₂ emissions since HTC-coal from biomass contains no

fossil carbon. Further experiments in this regard should also be carried out with the aim of reducing the carbon fraction in process water since this is virtually lost in terms of energy recovery. Treating possible toxic contaminants in process water from HTC such as phenols and ammonium as well as evaluating potential nutrient recycling applications for this highly concentrated phosphorus fertilizer should be also among the next steps to be taken. Identifying low-cost technologies to achieve both goals will be an important task in order to facilitate establishment of HTC technology.

ACKNOWLEDGEMENTS

Pascal Boivin, Alice Johannes, and Sylvain Melis are acknowledged for their SEM images and determination of the CEC in samples. Funding from the Swiss Commission for Technology and Innovation (CTI) is acknowledged (Project KTI-Nr. 11731.1 INNO-IW). Axel Funke and Felix Ziegler are thanked for providing data regarding molar ratios of carbonized samples from previous studies.

REFERENCES

1. Haszeldine, R.S., Carbon Capture and Storage: how green can black be? *Science*, Vol. 325, 2010, pp. 1647–1652.
2. Grimm, N.B., Faeth, S.H., Golubiewski, N.E., Redman C.L., Wu, J.G., Bai, X.M., Briggs, J.M., Global change and the ecology of cities. *Science*, Vol. 319, 2008, pp. 756–760.
3. Titirici, M.M., Thomas, A., Antonietti, M., Back in the black: hydrothermal carbonization of plant material as an efficient chemical process to treat the CO₂ problem. *New J Chem*, Vol. 31, 2007; pp. 787–789.
4. Funke, A., Ziegler F., Hydrothermal carbonization of biomass: A summary and discussion of chemical mechanisms for process engineering. *Biofuels Bioprod Biorefin*, Vol. 4, 2010, pp.160–177.
5. Rillig, M.C., Wagner, M., Salem, M., Antunes, P.M., George, C., Ramke, H.G., Material derived from hydrothermal carbonization: Effects on plant growth and arbuscular mycorrhiza. *Appl Soil Ecol*, Vol. 45, 2010, pp. 238–242.
6. Hu, B., Wang, K., Wu, L.H., Yu, S.H., Antonietti, M., Titirici, M.M., Engineering carbon materials from the hydrothermal carbonization process of biomass. *Adv Mater*, Vol. 22, 2010, pp. 813–828.
7. De Wit, J.N. 2001. *Lecturer's Handbook on whey and whey products*. Brussels: European Whey Products Association.
8. Smithers, G.W. Whey and whey proteins—From ‘gutter-to-gold’. *International Dairy Journal*, Vol. 18, 2008, pp. 695–704.
9. Ciesielski, H. and T. Sterckeman. Determination of cation exchange capacity and exchangeable cations in soils by means of cobalt hexamine trichloride. Effects of experimental conditions. *Agronomie*, Vol. 17, 1997, pp. 1–7.
10. Heilmann, S.M., Davis, H.T., Jader, L.R., Lefebvre, P.A., Sadowsky, M.J., Schendel, F.J. Hydrothermal carbonization of microalgae. *Bio-mass Bioenerg*, Vol. 34, 2010, pp. 875–882.
11. Bergius, F. Holz und Kohle, chemische und wirtschaftliche Betrachtungen. *Z Angew Chem*, Vol. 41, 1928, pp. 707–711.
12. Berl, E. and Schmidt, A. The behaviour of cellulose in pressure heating with water. *Justus Liebigs Annalen Der Chemie*, Vol. 461, 1928, pp. 192–220.
13. Berl, E. and Schmidt, A. On the Emergence of Carbon. III. The Incar-

- bonic Nature of Resin and Wax in a Neutral Medium. The Concept and Character of Bitumen. *Justus Liebigs Annalen Der Chemie*, Vol. 493, 1932, pp. 124–35.
14. Könnecke, H.G. and Leibnitz, E. Zur Kenntnis der Druckinkohlung von Braunkohlen in Gegenwart von Wasser. 2. *Journal für Praktische Chemie*, Vol. 1, 1955, pp. 200–208.
 15. Leibnitz, E., Könnecke, H.G., Lietz, L. Zur Kenntnis der Druckinkohlung von Braunkohlen in Gegenwart von Wasser. 3. *Journal für Praktische Chemie*, Vol. 5, 1957, pp. 97–100.
 16. Leibnitz, E., Könnecke, H.G., Schröter, M. Zur Kenntnis der Druckinkohlung von Braunkohlen in Gegenwart von Wasser. 4. *Journal für Praktische Chemie*, Vol. 6, 1958, pp. 18–24.
 17. Davis, A. and W. Spackman. Role of cellulosic and lignitic components of wood in artificial coalification. *Fuel*, Vol. 43, 1964, pp. 215–217.
 18. Geissler, C. and L. Belau. Behaviour of stable carbon isotopes during coalification. *Z Angew Geol*, Vol. 17, 1971, pp. 13–17.
 19. Li, R.X., Jin, K.L., Lehrmann, D.J. Hydrocarbon potential of Pennsylvanian coal in Bohai Gulf Basin, Eastern China, as revealed by hydrous pyrolysis. *Int J Coal Geol*, Vol. 73, 2008, pp. 88–97.
 20. Sevilla, M. and A.B. Fuertes. The production of carbon materials by hydrothermal carbonization of cellulose. *Carbon*, Vol. 47, 2009, pp. 2281–2289.
 21. Suggate, R.P. Analytical variation in Australian coals related to coal type and rank. *Int J Coal Geol*, Vol. 37, 1998, pp.179–206.
 22. Hunt, J.M. 1995. *Petroleum geochemistry and geology*. San Francisco: W.H. Freeman.
 23. Schor, F. Mit dem Rindvieh Schotte verwerten. Merkblatt für die Praxis. *ALP aktuell* Vol. 35, 2009, Eidgenössisches Volkswirtschaftsdepartement EVD; Forschungsanstalt Agroscope Liebefeld-Posieux ALP.
 24. AWEL. Kompostier- und Vergärungsanlagen im Kanton Zürich. *Statistik info* Vol. 19, 1998, www.statistik.zh.ch/themenportal/themen/down.php?id=135&fn=1998_19.pdf (Access: December 2010).
 25. Graber, A. and R. Junge-Berberović. Wastewater-fed Aquaculture Otelfingen, Switzerland: Influence of system design and operation parameters on the efficiency of nutrient incorporation into plant biomass. In: Vymazal J., editor. *Wastewater Treatment, Plant Dynamics and Management in Constructed and Natural Wetlands*: Springer Verlag; 2008, pp. 299–310.
 26. Graber, A., Junge, R., Skvarc, R. Elimination of phenols, ammonia and cyanide in wash water from biomass gasification, and nitrogen recycling using planted trickling filters. *Water Sci Technol*, Vol. 60, 2010, pp. 3253-3259. DOI:10.2166/wst.2009.728.
 27. KLZH. 2009. *Kantonales Labor Zürich. Für Trinkwasser gültige Toleranz-, Grenz- und Erfahrungswerte*. Zürich; www.klzh.ch/downloads/werte_tw.pdf (Access: December 2010).
 28. GSchV. 1998. *Gewässerschutzverordnung*, SR 814.201, Bern.
 29. Hui, Y.H. 2007. *Handbook of food products manufacturing*. New Jersey: John Wiley & Sons.

Preparation of High-Specific Surface Area-Activated Carbon with Oil-Bearing Mud Residue

YUE MA*, MIAN CHEN and YAN JIN

State Key Laboratory of Petroleum Resources and Prospecting, China University of Petroleum, Beijing 102249, People's Republic of China

ABSTRACT: Oil-bearing mud residue is a hazardous waste composed of minerals, mineral oil, and water. It is characterized by a high yield and a high content of heavy oil. It is not comprehensively utilized and is difficult to process. The primary sources are oil sludge and oil sand from petroleum exploration and development and from petrochemical production. Oil-bearing mud residue is declared a hazardous waste by Chinese law. Thus, its treatment and application is a problem requiring an immediate solution for petroleum and petrochemical industries. Using oil-bearing mud residue as feedstock and NaOH as the activator this study demonstrates production of activated carbon with high specific surface area. Features of this activated carbon include a specific surface area up to 2,700 m²/g and even pore size. Average pore size is less than 2 nm and total pore volume exceeds 2 cm³/g. This method provides a new approach for recycling oil-bearing mud residue.

INTRODUCTION

As an active absorbent material, activated carbon is used widely and in great demand. However, specific surface area and total porous volume of conventional activated carbon are usually 800–1,500 m²/g and 0.5–1.0 cm³/g, respectively, and are far below demands for environmental protection. Currently, activated carbon with high specific surface area is used as an energy storage medium for hydrogen, natural gas, and electricity; as electrode material for electrochemical capacitors; as an efficient adsorption agent for poisonous gases; as a filler for chromatographic columns; as catalyst carriers, and more in cases where conventional activated carbon is not sufficient. Consequently, research and development into high-specific surface area-activated carbon processes have increasingly attracted attention from scientific and technical researchers [1,2,3,4]. Developed countries such as Japan and the United States have successfully produced activated carbon with a specific surface area of more than 2000 m²/g at a price of 85–1 million RMB/ton with petroleum coke and coal tar as feedstocks. Its demand in China depends primarily on import availability. In addition, research into preparation of this material is still in the early stages of experimentation and inves-

tigation. Feedstocks include petroleum coke, coconut shell, bamboo, and more [5,6,7]. Preparation of high specific surface area-activated carbon using oil-bearing sludge as a feedstock has not been published in literature around the world.

Oil-bearing mud residue is a hazardous waste. Its primary components are minerals, mineral oil, and water. Characterized by a high yield, high content of heavy oil, it is less comprehensively utilized and difficult to process [8,9]. Its primary source is oil sludge and oil sand from petroleum exploration and development and from the petrochemical production industry. Using oil-bearing mud residue as feedstock and NaOH as the activator a method is provided to produce activated carbon with high specific surface area. This method both disposes of oil sludge and re-uses waste.

EXPERIMENTS

Experimental Materials and Instruments

This study analyzes the reaction of oil-bearing mud residue and A.R. level NaOH from the Beijing Chemical Plant. Experimental instruments employed include an SRJX-4-13 box resistance furnace (Beijing ever light medical equipment Co, LTD), an indoor static pyrolysis oven (constructed on-site), a Quantax 200× Flash 5000–10× X-ray energy spectrometer (FEI Hong Kong, LTD), a Quanta 250 scanning electron mi-

*Author to whom correspondence should be addressed.
E-mail: mayue0327@163.com

croscope with a tungsten filament (Bruker AXS Corporation, Germany), a NOVA-2000e fully automatic specific surface and porosity analyzer (Quantachrome, USA), and a STA449F3 simultaneous thermal analyzer (NETZSCH-Gerätebau GmbH, Germany).

Experimental Procedure

High-specific surface area-activated carbon is prepared using airtight dry distillation and high-temperature activation. Experiment procedures were as follows:

1. The oil-bearing mud residue is mechanically dehydrated.
2. At a specified temperature and under a nitrogen barrier, the dehydrated residue is dry-distilled at a carbonizing temperature of 320–500°C.
3. The carbide is de-ashed to remove its ash content.
4. The de-ashed carbide is mixed with the activator, and the mixture is activated at 320–900°C under the nitrogen barrier.
5. The activated products are ground, washed to neutral and dried at 120°C.

Sample Characterization

After desorption at 150°C and 1.33 Pa in the surface area and porosity automatic analyzer (NOVA-2000e) for 4 hrs. The N₂ adsorption isotherm of the sample is measured. Then, specific surface area and pore size distribution are determined using the BET method. Sample components are analyzed qualitatively with assistance of 200× Flash 5000-10× X-ray spectroscopy. The microstructure of the sample was viewed using a Quanta 250 scanning electron microscope in tungsten filament mode.

RESULTS AND DISCUSSION

Effect of Preparation Parameters on the Performance of Activated Products

Preparation of activated carbon can be divided into two stages: (1) Carbonization of feedstock. The purpose of carbonization is to obtain carbonized material with an initial porosity and mechanical strength. This material is suitable for activation which is virtually pyrolysis of the organic matter in the feedstock including thermal decomposition and polycondensation [10] and

(2) Activation of the carbonized material. This is the key process during preparation of activated carbon. It is a series of complex chemical reactions between the activator and carbonized material. Activation is characterized by formation of new pores based on initial pores, extension of the initial pores, and merging and connection between pores [11]. Effects of carbonization of feedstock and activation parameters on performance of activated products are discussed below.

Influence of Carbonization Temperature

Composition of oil-bearing mud residue is complicated. Analyses of mud residue from oilfields display the following ranges (W/W) in composition: 15–30% oil, 60–70% water, and 10–15% residue. Preparation of activated carbon requires a set carbonization temperatures. Thus, water, organic matter, and volatile matter in residue may be removed during carbonization resulting in carbonized material with an initial porosity and mechanical strength ready to be activated. The thermal gravimetric curve of the oil-bearing sludge from an oilfield is obtained by a STA449F3 simultaneous thermal analyzer as displayed in Figure 1.

Data in Figure 1 display that the process of carbonization occurs in three stages: volatilization of water and light oil (40–140°C), thermal decomposition (140–410°C), and polycondensation (410–500°C). When temperature exceeds 500°C, the weight loss of feedstock is small indicating the carbonization process stops. Change of iodine adsorption in carbide as a function of carbonization temperature is displayed in Table 1.

Data in Table 1 show that when the carbonization

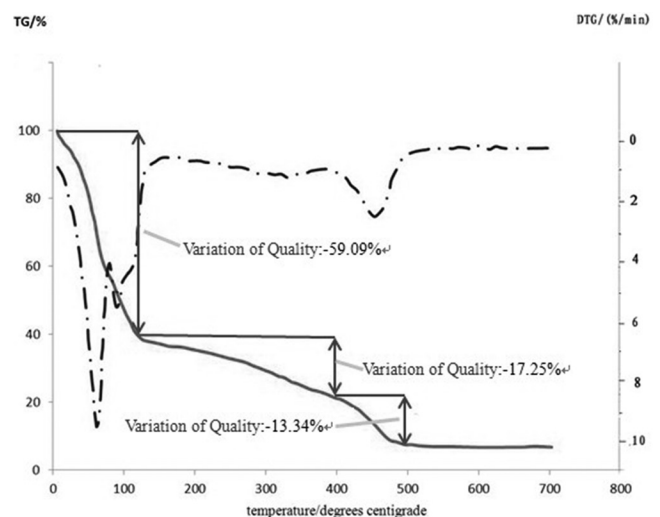


Figure 1. Thermal gravimetric analysis curve of oil-bearing sludge.

Table 1. Effect of Carbonization Temperature on Adsorption Performance of Carbide.

Carbonization Temperature (°C)	Carbide	
	Carbon Content, w%	Iodine Adsorption, mg/g
450	45.2	300.6
500	46.6	357.4
550	46.0	291.0
600	45.8	256.3

temperature exceeds 500°C, despite slight decrease in carbon content, the iodine adsorption value is dramatically reduced. This implies that an increase in carbonization temperature will damage the internal structure [12], affect initial pore formation, and reduce adsorption performance. Therefore, appropriate carbonization temperature must be determined for each type of oil-bearing mud residue.

Effects of Activation Heating Mode

Activation heating modes tested are as follows:

- Continuous heating from room temperature to activation temperature (i.e., feedstock is placed into pyrolysis furnace at room temperature);
- Rapid heating from room temperature to activation temperature (i.e., feedstock is placed directly into high temperature pyrolysis furnace); and
- Pre-activation at low temperature and activation at high temperature. After one hour activation at 800°C [$m(\text{NaOH})/m(\text{C}) = 2$] the effect of the heating mode on specific surface area of the activated product is measured. Results are displayed in Table 2.

Data in Table 2 show that activation mode (c) is the only method that yields a product with high specific surface area and good data stability and repeatability. That is because the rapid heating of modes (a) and (b) cause the NaOH to dehydrate rapidly. The system then

Table 1. Effect of Heating Mode on Specific Surface Area of Activation Product.

Heating Mode	Specific Surface Area (m ² /g)		
	First Time	Second Time	Third Time
a	2176	1853	2201
b	1326	1589	1477
c	2720	2780	2755

expands causing uneven thermal conductivity. Thus, the activator and carbide cannot fully contact to react well leading to poor repeatability and low specific surface area. Before heating to activation temperature mode (c) pre-activates at 320°C and the activated product has good repeatability and reliability. It may be because 318°C is the melting point of NaOH, such that NaOH is completely dehydrated and the reactants are well distributed. Thus, no expansion phenomenon occurs at that point.

Influence of Activation Temperature

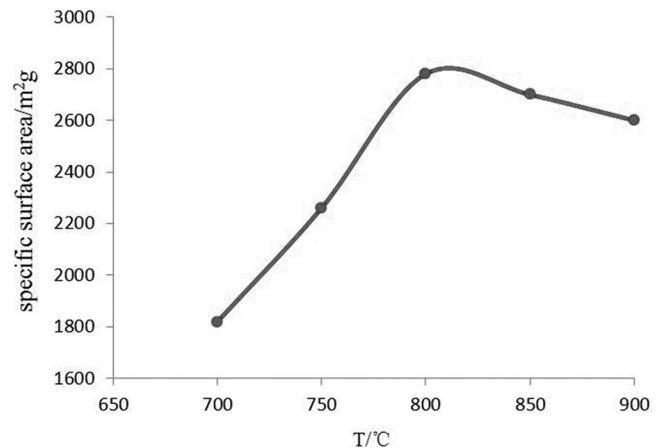
Using the condition $m(\text{NaOH})/m(\text{C}) = 2$ and activating for 1 hr, the relation curve between temperature and specific surface area of activated carbon is displayed in Figure 2.

Optimum activation temperature is approximately 800°C as displayed in Figure 2. If the activation temperature is too low the activation reaction cannot be completed and if it is too high the reaction will be excessively aggressive causing pore walls to burn to the point of collapse and thus reducing specific surface area. Therefore, there is an optimal temperature for activating this reaction.

Influence of Activation Time

Effect of activation time on specific surface area of activated carbon for conditions $m(\text{NaOH})/m(\text{C}) = 2$ and activation temperature 800°C was analyzed. Results are displayed in Figure 3.

The optimal activation time is approximately 1 h. As the activation time increases, the specific surface area of activated carbon first increases and then decreases.

**Figure 2. Effect of activation temperature on specific surface area of activated carbon.**

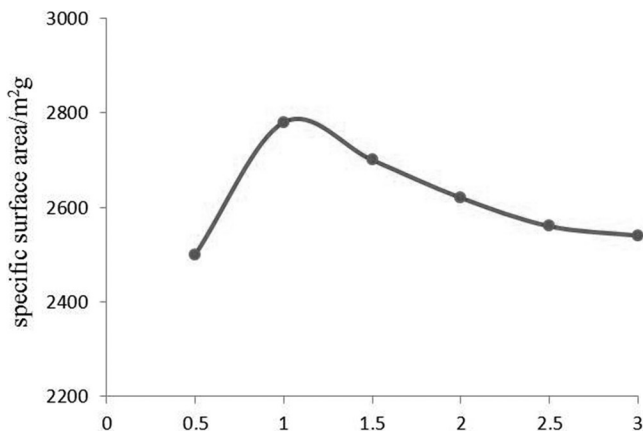


Figure 3. Effect of activation time on specific surface area of activated carbon.

As the reaction time and depth increase, the number of micropores increases before the specific surface area reaches its maximum value. When the specific surface area reaches its maximum, the number of micropores also reaches its maximum. If the activation time is extended past this maximum, the micro-pore walls will fall down, and large numbers of micropores will melt into mesopores and macropores, resulting in a decrease in specific surface area [13].

Influence of Alkali/Carbon Ratio

The effect of $m(\text{NaOH})/m(\text{C})$ on specific surface area of activated carbon at an activation temperature of 800°C for 1 hour is measured and the results are displayed in Figure 4. As $m(\text{NaOH})/m(\text{C})$ increases, the specific surface area of activated product increases significantly. However, when this ratio reaches 2, the surface area changes slowly and shows a tendency to decrease with continued increase of the ratio. Carbonized material and amorphous carbon in the cracks are acti-

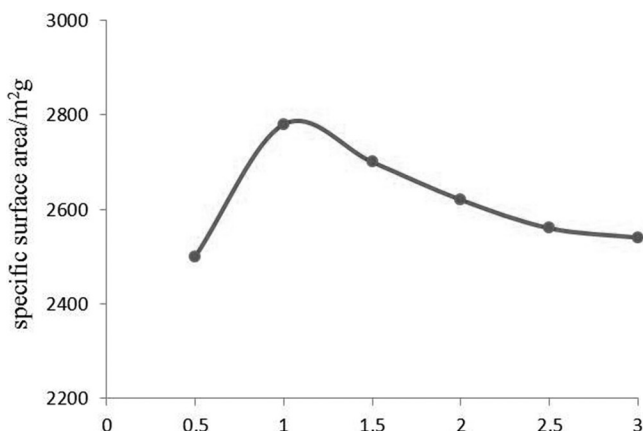


Figure 4. Effect of $m(\text{NaOH})/m(\text{C})$ on specific surface area of activated carbon.

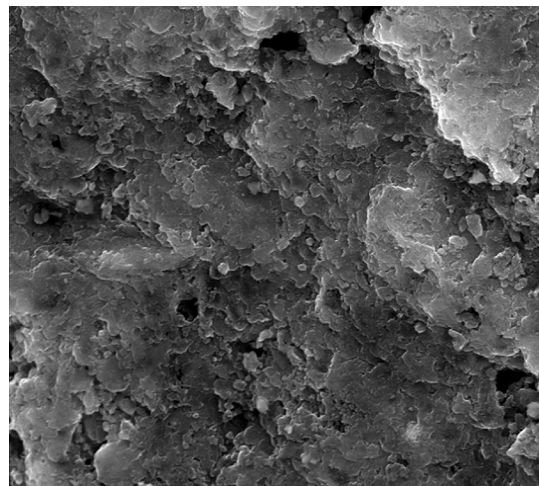


Figure 5. Scanning electron microscope picture of carbide.

ated first, and a microporous structure is formed. As the amount of NaOH increases, both the reaction speed and the number of micropores in the carbonized material increase, thus increasing the specific surface area. As $m(\text{NaOH})/m(\text{C})$ continues to increase, the reaction between excess NaOH and intervals of the carbon atom layer of the formerly generated microporous structure cause the carbon material to over-ablate and pore size increases; thus, specific surface area decreases slightly.

Analysis and Discussion of Scanning Electron Microscope (SEM) and Porosity

The micro morphology of the activated carbon surface is viewed using a scanning electron microscope (SEM). The features of its surface morphology before and after activation are displayed in Figures 5 and 6, respectively.

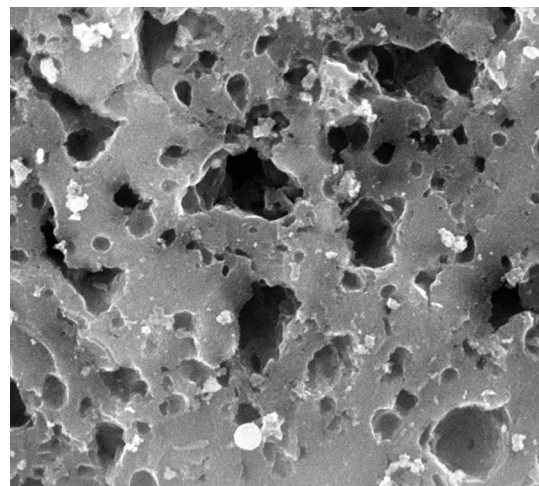


Figure 6. Scanning electron microscope picture of activation product.

Table 3. Oil-bearing Sludge Adsorption Characterization of Carbonization and Activation Product.

Sample Name	Specific Surface Area (m ² /g)	Average Pore Size (nm)	Total Pore Volume (ml/g)	Micropore Volume 0–2 nm (ml/g)	Mesopore Volume 2–35 nm (ml/g)	Large Pore Volume >35 nm (ml/g)	Micropore Proportion (%)
Activated products	2780	1.66	2.13	0.74	0.39	0.368	49.4
Commercial activated carbon	941.2	2.123	0.1234	0.0380	0.082	0.0034	30.8

The image displayed in Figure 5 reveals a flaky surface for the oil-bearing mud residue that is nearly free of pores only containing a few cracks. The picture of the activated carbon sample displayed in Figure 6, however, shows abundant pore structures on the surface of the particles. Only large pores can be seen, but the large pores provide the necessary sites for the numerous internal micro-pore structures in the activated carbon whose existence are proven by the adsorption characteristics of the activated product displayed in Table 3. Compared with conventional commercial activated carbon, activated carbon prepared in this manner performs better both in specific surface area and porosity distribution. The conclusion is that the carbonized oil-bearing mud residue is corroded and abundant pore structures are formed through a redox process [14,15,16].

CONCLUSIONS

Using oil-bearing mud residue as feedstock and NaOH as the activator, activated carbon with a specific surface area up to 2,780 m²/g was prepared for specific conditions of activation mode, $m(\text{NaOH})/m(\text{C})$ ratio, activation temperature, and activation time. This product has a high percentage of micropores, low average pore size, and large specific surface area. This study provides a method for a new approach useful for recycling oil-bearing mud residue.

ACKNOWLEDGEMENTS

Authors are grateful for project support from the National Natural Science Foundation of China (No.51234006) and financial support from Major National Science and Technology Project (No.2011ZX0500900501B).

REFERENCES

1. GC Grunewald and RS Drago. Carbon molecular sieves as catalysts

- and catalyst supports. *J. Am. Chem. Soc.*, Vol. 113, No.5, 1991, pp. 1636–1639.
2. Wennerberg et al. Active carbon process and composition: US Patent. Patent No.4082694, 1978.
3. D. Lozano-Castelló, M.A. Lillo-Ródenas, D. Cazorla-Amorós, A. Linares-Solano. Preparation of activated carbons from Spanish anthracite: I. Activation by KOH. *J. Carbon*, Vol 39, No. 5, 2001, pp. 741–749.
4. Hsisheng Teng, Yao-Jen Chang, Chien-To Hsieh., Performance of electric double-layer capacitors using carbons prepared from phenol-formaldehyde resins by KOH etching. *J. Carbon*, Vol. 39, No. 13, 2001, pp. 1981–1987.
5. M.A Lillo-Ródenas, D Lozano-Castelló, D Cazorla-Amorós, A Linares-Solano., Preparation of activated carbons from Spanish anthracite II. activation by KOH[J]. *J. Carbon*, Vol. 39, No. 5, 2001, pp.751–759.
6. J. Diaz-Terána, D.M. Nevskaja, J.L.G. Fierro, A.J. López-Peinado, A. Jerez. „Study of chemical activation process of a lignocellulosic material with KOH by XPS and XRD. *J. Microporous and Mesoporous Materials*, Vol. 60, No. 1–3, 2003, pp.173–181.
7. M.A Lillo-Ródenas, D Cazorla-Amorós, A Linares-Solano., Understanding chemical reactions between carbons and NaOH and KOH: An insight into the chemical activation mechanism. *J. Carbon*, Vol. 41, No. 2, 2003, pp. 267–275.
8. Lu Yunhu, Chen Mian, Jin Yan., The development and application of an environmentally friendly encapsulator EBA-20. *J. Petroleum Science & Technology*, Vol. 30, No. 21, 2012, pp. 2227–2235.
9. U.S. Environmental Protection Agency, Office of Solid Waste and Emergency. 1998. Final Standards Promulgated for Petroleum Refining Waste, U.S. Environmental Protection Agency, Office of Solid Waste and Emergency Response, Washington, DC.
10. E Raymundo-Piñero, D Cazorla-Amorós, A Linares-Solano., Structural characterization of N-containing activated carbon fibers prepared from a low softening point petroleum pitch and a melamine resin. *J. Carbon*, Vol. 40, No. 4, 2002, pp. 597–608.
11. Ruowen Fu, Ling Liu, Wenqiang Huang, Pingchun Sun., Studies on the structure of activated carbon fibers activated by phosphoric acid, *J. Journal of Applied Polymer Science*, Vol. 87, No. 14, 2003, pp. 2253–2261.
12. M Molina-Sabio, F Rodriguez-Reinoso., Role of chemical activation in the development of carbon porosity. *J. Colloids and Surfaces A: Physicochemical and Engineering Aspects*, Vol. 241, No.1–3, 2004, pp. 15–25.
13. Paul T Williams, Anton R Reed., Pre-formed activated carbon matting derived from the pyrolysis of biomass natural fibre textile waste. *J. Journal of Analytical and Applied Pyrolysis*, Vol. 70, No. 2, 2003, pp. 563–577.
14. A. Gil, G.de la Puente, P. Grange., Evidence of textural modifications of an activated carbon on liquid-phase oxidation treatments. *J. Microporous Materials*, Vol. 12, No. 1–3, 1997, pp. 51–61.
15. Douglas W. McKee, Clifford L. Spiro, Philip G. Kosky, Edward J. Lamby., Eutectic salt catalysts for graphite and coal char gasification. *J. Fuel*, Vol. 64, No. 6, 1985, pp. 805–809.
16. José J. Pis, Teresa A. Centeno, Manuel Mahamud., Preparation of active carbons from coal Part I. Oxidation of coal. *J. Fuel Processing Technology*. Vol. 47, No. 2, 1996, pp. 119–138.